From the graph of Figure 48 you notice a significant improvement of the shielding factor with respect to the previous cases. In general the values of SF are grown in all the points of the three inspection lines closest to the ground and especially the SF remains high even in the points which are not in direct correspondence of the screen.

A different assessment must be made for the values calculated to the share of 2 m. In this case the shielding factor drops compared to the previous cases, and this is probably due to a shift of the end effect of the shield.

- Shielding u-shaped rear closed

In order to verify the influence of the ferromagnetic material not directly interposed between the source and the victim, the configuration u-shaped has been tested even with the open part on the victim side.
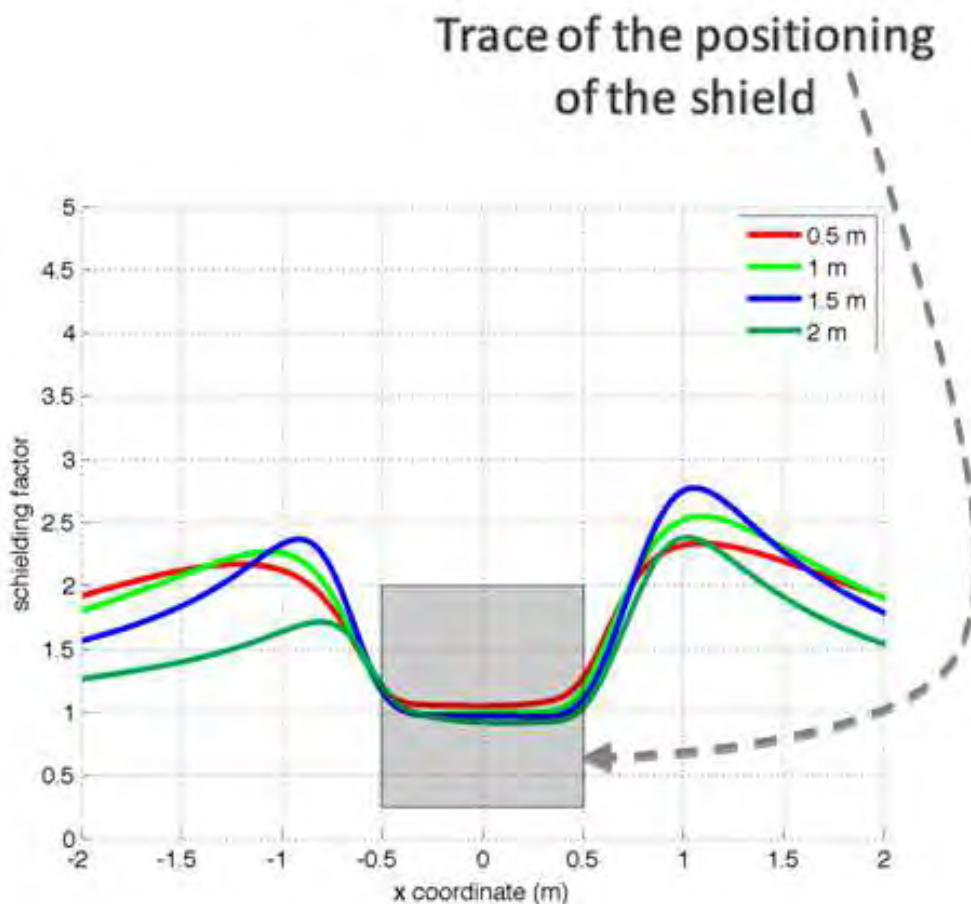

Figure 49 Shielding factor provided by u- shaped shield rear closed

From the graph of Figure 49 it is clear that the shielding system work in the correct way only for the shielding of the value of magnetic induction generated on the sides of the electrical cabinet. The values of the shielding factor on the front of the electrical cabinet, on every computation lines are close to 1 and so this kind of shielding system can be proposed only on the case in which only the sides have to be shield.

- Shielding closed on all 4 sides

Finally the solution shielded on four sides has been presented. This solution usually guarantees the best shielding factors but in practical applications it is almost never used as it turns out to be also the most expensive.
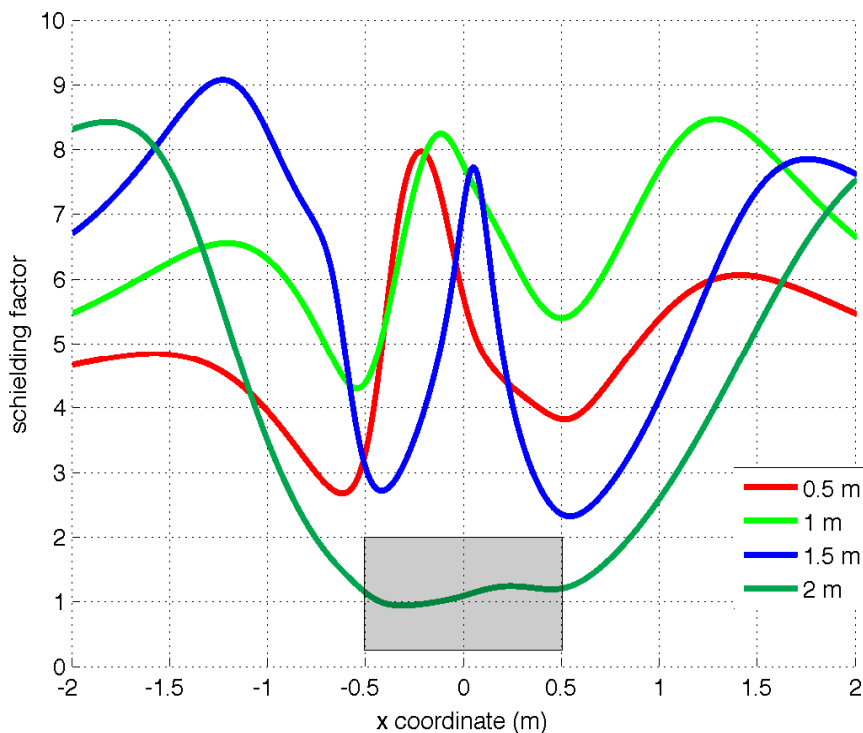

Figure 50 Shielding factor of the solution closed on all four sides

From the Figure 50 it's clear that this solution provide the highest values of shielding factor in all the points of the three inspection lines closest to the ground, the values obtained are also doubled compared to the best solutions previously tested. In contrast, even this solution has problems due to the end effect on the inspection line at 2 m. These end effect are not noticed on the line at 0.5 m as the source field has a different direction, in fact the computation line at 0.5 m is if front at the center point were the currents have a different direction.

4.2.3   Conclusion

Evaluated the results presented in the previous section it can be said that the best solution is that closed on 4 sides. The owner of the electrical cabinet has decided to install the solution composed of only two plates as it is less expensive and can guarantee, although with a safety coefficient relatively low, the respect of the established objective. Took note of the decision of the house owner was also examined whether the use of a material thinner and more powerful would ensure greater safety coefficient. is why it was decided to test a solution composed of two sheets of material with the following properties:

- relative magnetic permeability μ_r= 20000
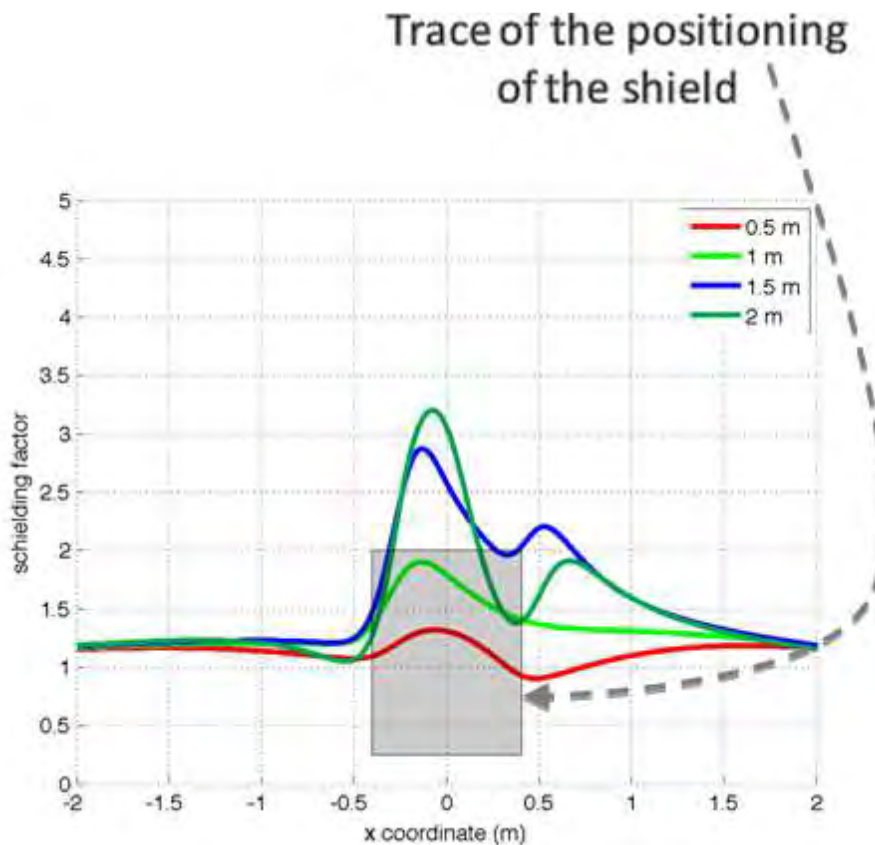- thickness of 0.2 mm

Figure 51 Shielding factor provided by the two plates positioned in front with a different material

The results obtained with the last solution presented in Figure 51 provide a slight improvement in the values of shielding factor on all computing lines with exception of that at 2 m. Being the values of magnetic induction higher in correspondence of the line computing to 1 m is chosen so to favor the solution that guarantees a better shielding factor at this height and consequently the one with material with a higher magnetic permeability.

4.3 Shielding of a public office under a substation MV/LV

In this chapter a conductive shield system is presented. The objective is the reduction of values of magnetic induction more than 3 μT in a public office that have to be realized under a MV/LV substation.

The layout of the substation with the position of the component and the low voltage power lines is presented in Figure 52.
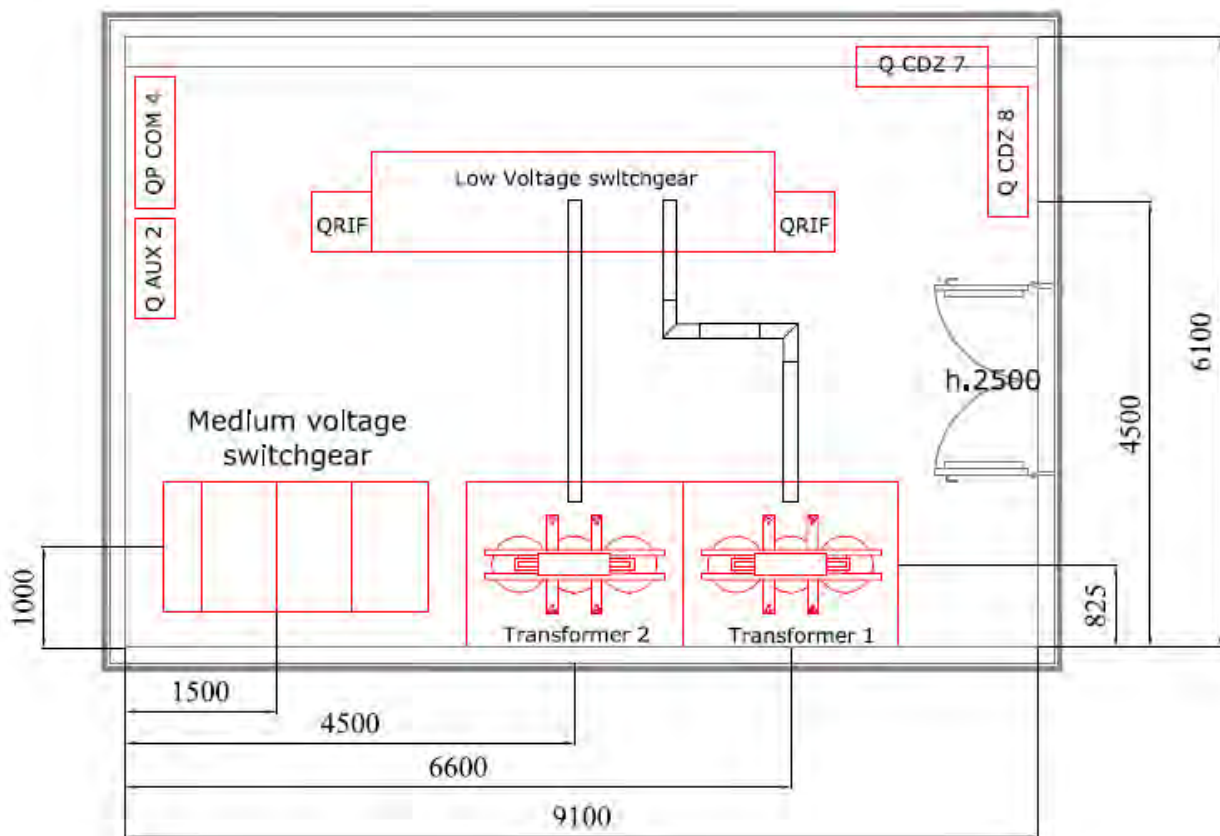

Figure 52 Layout of the substation with the position (in mm) of the component

The substation consists of

- Two cast resin transformers MV/LV with power of 2000 kVA
- A low voltage switchgear consisting of four compartments
- A medium voltage switchgear consisting of four compartments
- Two low voltage power lines composed of busbar with rated current equal to 3200 A

- Two medium voltage power lines

The two transformer never work simultaneously but it is not possible to know which one will be activated and so the shielding system has to be design in order to protect from the magnetic induction generate from each transformer.

4.3.1 Computation of the values of magnetic induction produced by the substation

In this application the modellization of the source is more difficult than in the previously application because there are different sources on the substation. The sources have been simulated taking into account their relative position.

All simulations will be performed obtaining the current of each unit from the rated power of the transformer. With this data and taking into account the primary and secondary voltages of the transformer is possible to obtain the incoming current from the medium voltage switchgear and departing to the Low voltage switchgear.

Obtained this data is possible derive, by studying the internal layouts of the switchgears, the current path and evaluate the current share allocated to each compartment of the switchgear.

The internal slash of each switchgear has been faithfully reproduced from the data provided by the manufacturer.

The busbar connection between the transformers and the LV switchgear have been simulated as a power line with the cables arranged as the internal bars of the busbar.

The complete model of the electrical substation is presented in Figure 53.

As stated above the two transformers never work simultaneously and consequently it is necessary to study two different cases, the first with only the transformer 1 active, and the second with the only transformer 2 active. The shielding system must, however, be designed to protect the staff office if any of the two transformers will be active.

In this elaborate only the results obtained with the transformer 1 active will be take into account as the results of the two analyzes turn out to be very similar and their presentation for the Transformer 2 would be a needless repeat.

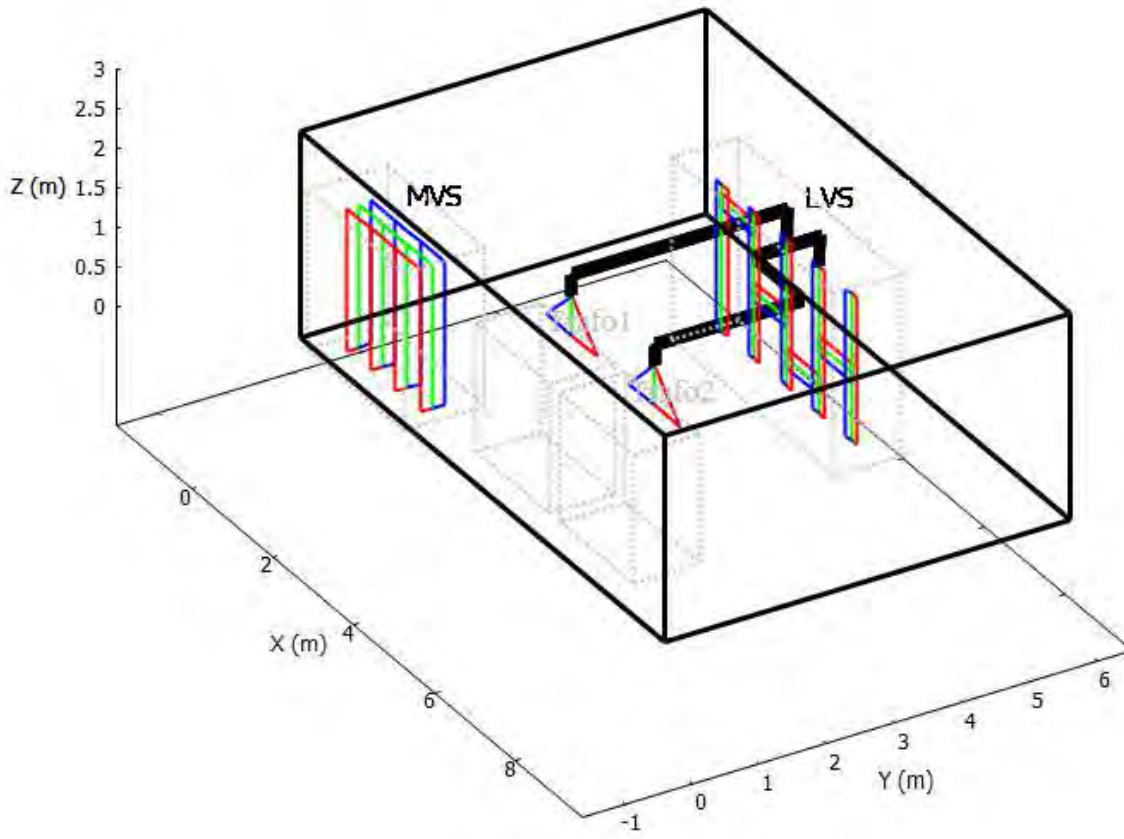The layout of the substation with only the transformer one active is presented in Figure 54

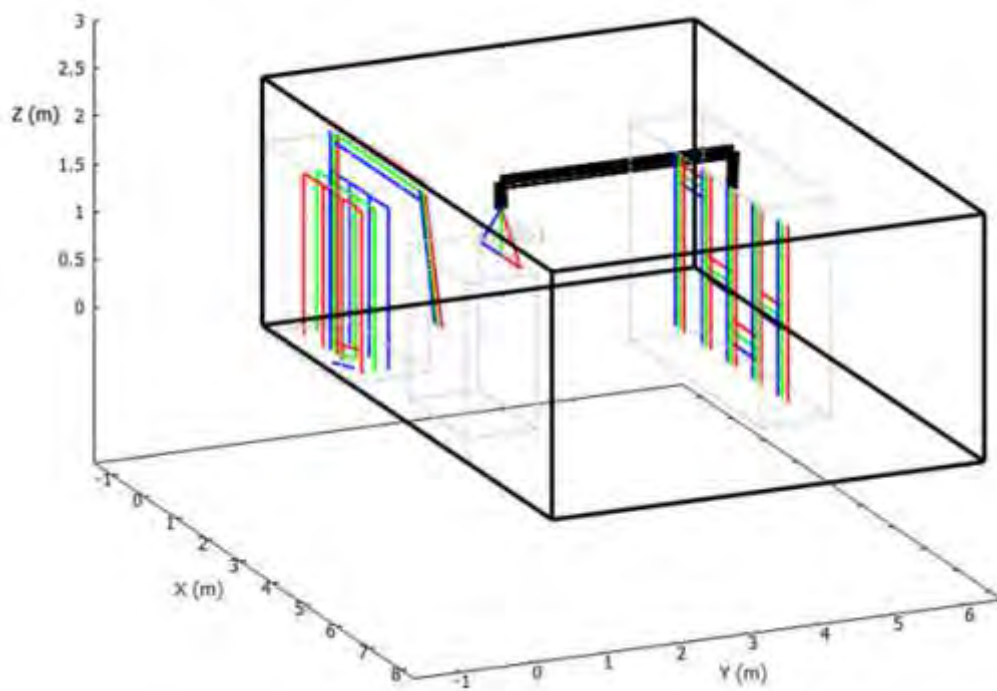**Figure 53 Complete model of the electrical substation**

Figure 54 Model of the substation with only transformer 1 active

In this case, the offices are positioned below the electrical substation and the target is not exceeded the value of 3μT in all over a volume below the substation between the height of z = -3 m and z= -1.6 m respect to the floor of the substation.

The values of magnetic induction calculated at the height of -1.6 m and -3 m are presented respectively in Figure 55 and in Figure 56 the black line outline represent the projection of the perimeter of the substation on the computation plane.
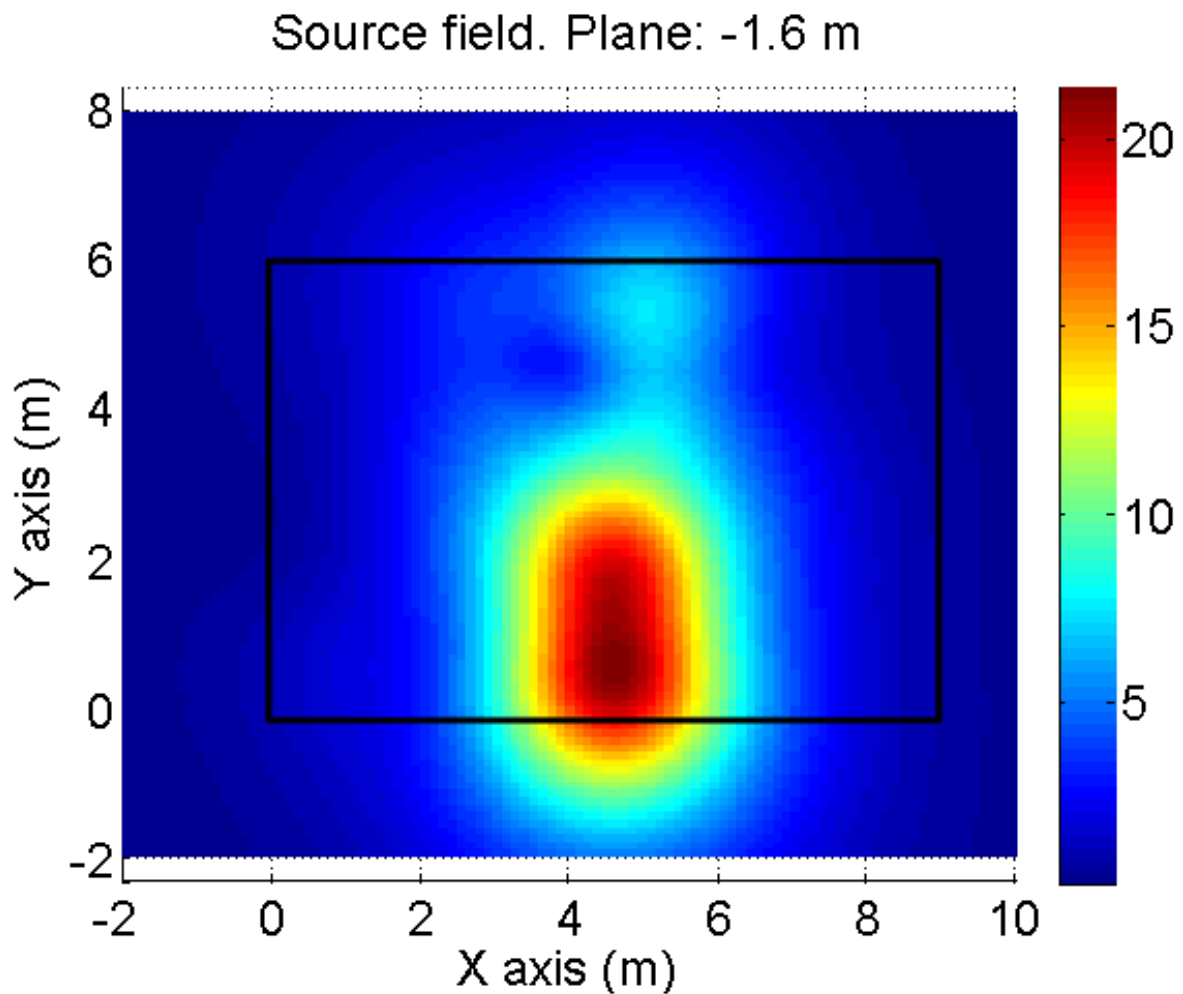

Figure 55 field map of the magnetic induction calculated on an xy plane with height z equal to -1.6 m
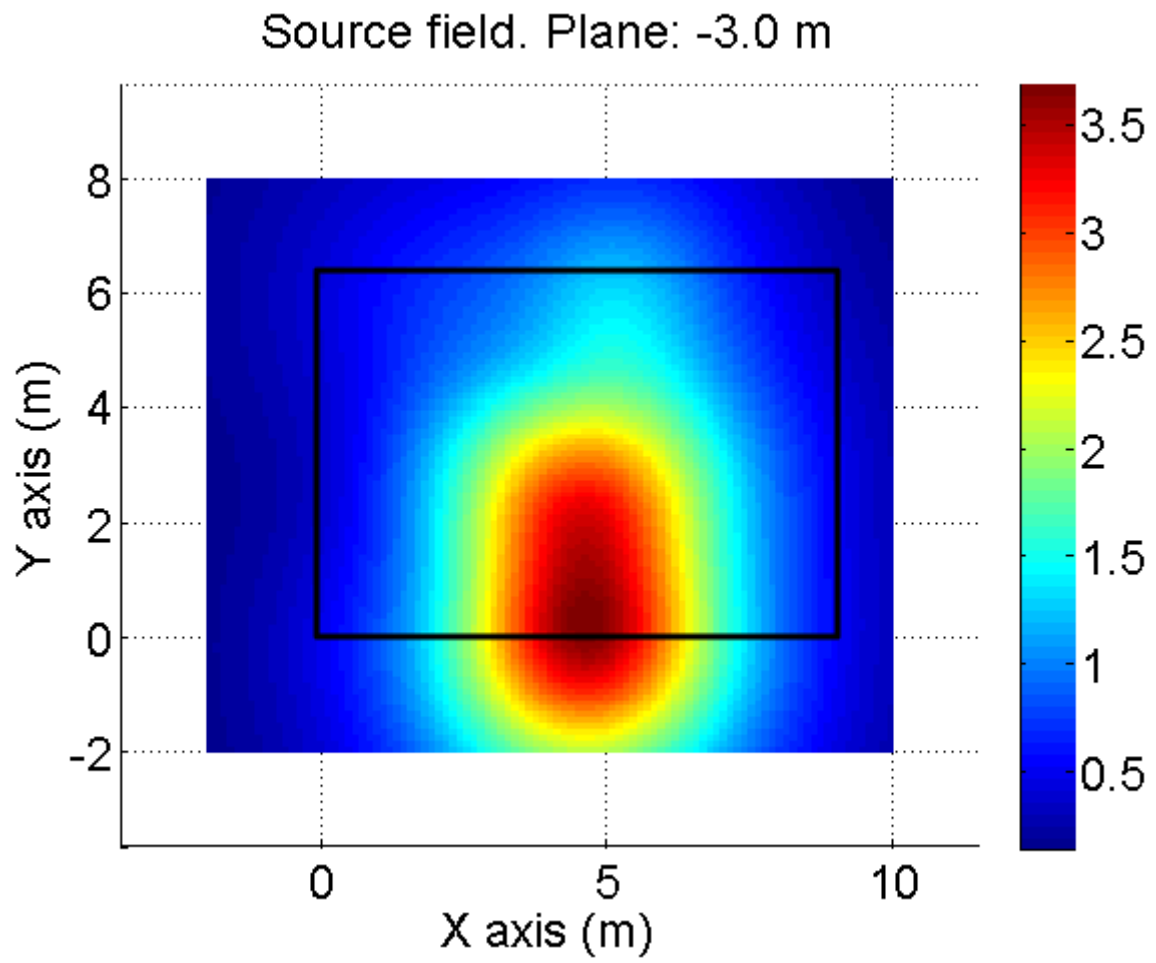
Figure 56 field map of the magnetic induction calculated on an xy plane with height z equal to -3 m

4.3.2 Design of the shielding system

For this application the design of the shielding system was carried out using a conductive material. In particular it was supposed to a big part of the floor of the substation with slabs of aluminum. In order to attenuate the end effect of the shield was also provided an appendix to the wall rear the transformer.

For the simulation has been take into account the property of the material listed below:

- Electrical conductivity = 35 MS/m
- Relative magnetic permeability $\mu_r = 1$
- Thickness of the slabs = 3 mm
- Area of the shielding system = 40.5 m^2

The layout of the shielding system and the relative position of the sources and of the computation planes (z = -1.6m) is presented in Figure 57:
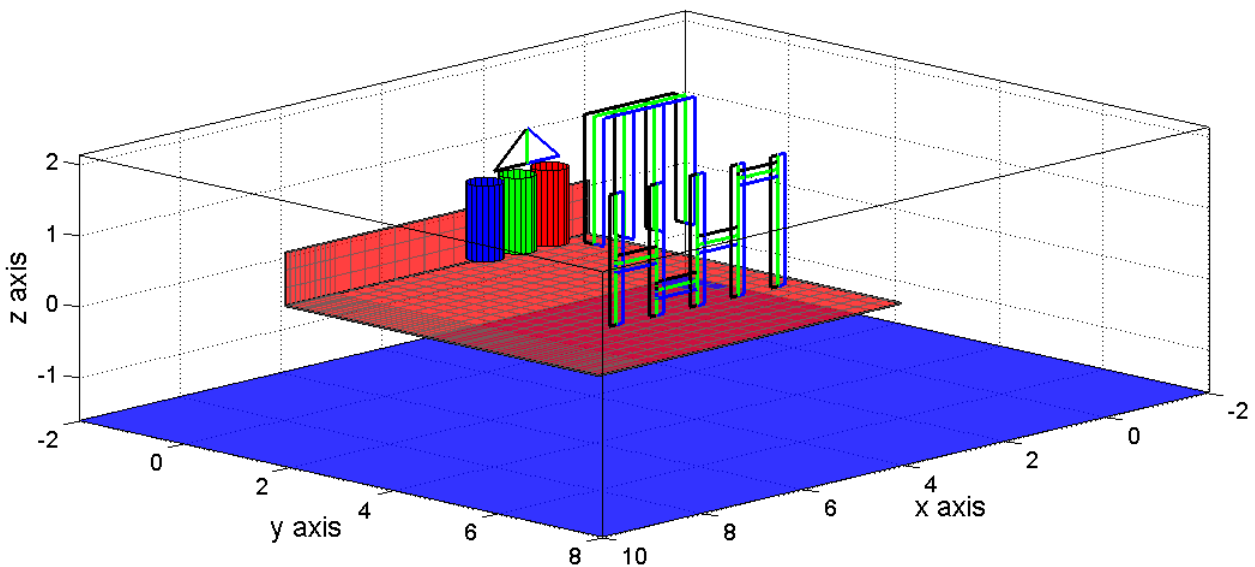

Figure 57 Layout of the shielding system with the relative position of the source and of the computation plane

In Figure 57 are present: the shielding system in red, the computation plane in blue and the other the devices of the substation. The Medium voltage switchgear is crossed by relatively low values of current (max. 50 A) and so not generate high values of magnetic induction and is and it is not necessary that the shielding system is installed below it.

4.3.3 Result of the simulations

The simulations was carried out using the data listed below. Clearly if the values of magnetic induction at the height of z=-1.6 will be less than 3 μT then surely, at the height of z = -3 m and at all intermediate heights, they will be less than the value of 3 μT. It is however still interesting to show the results obtained at z = -3 m to analyze the variation of the SF moving away from the shield.

The first result obtain with the simulation is are the eddy current induced on the shielding system. The eddy current depend only on the geometry of the screen and from the sources of magnetic induction and therefore turn out to be the same for both the calculation plane z = -1.6 m than to z = -3 m.

In Figure 58 and in Figure 59 are represented respectively the real part and the imaginary of the eddy currents.
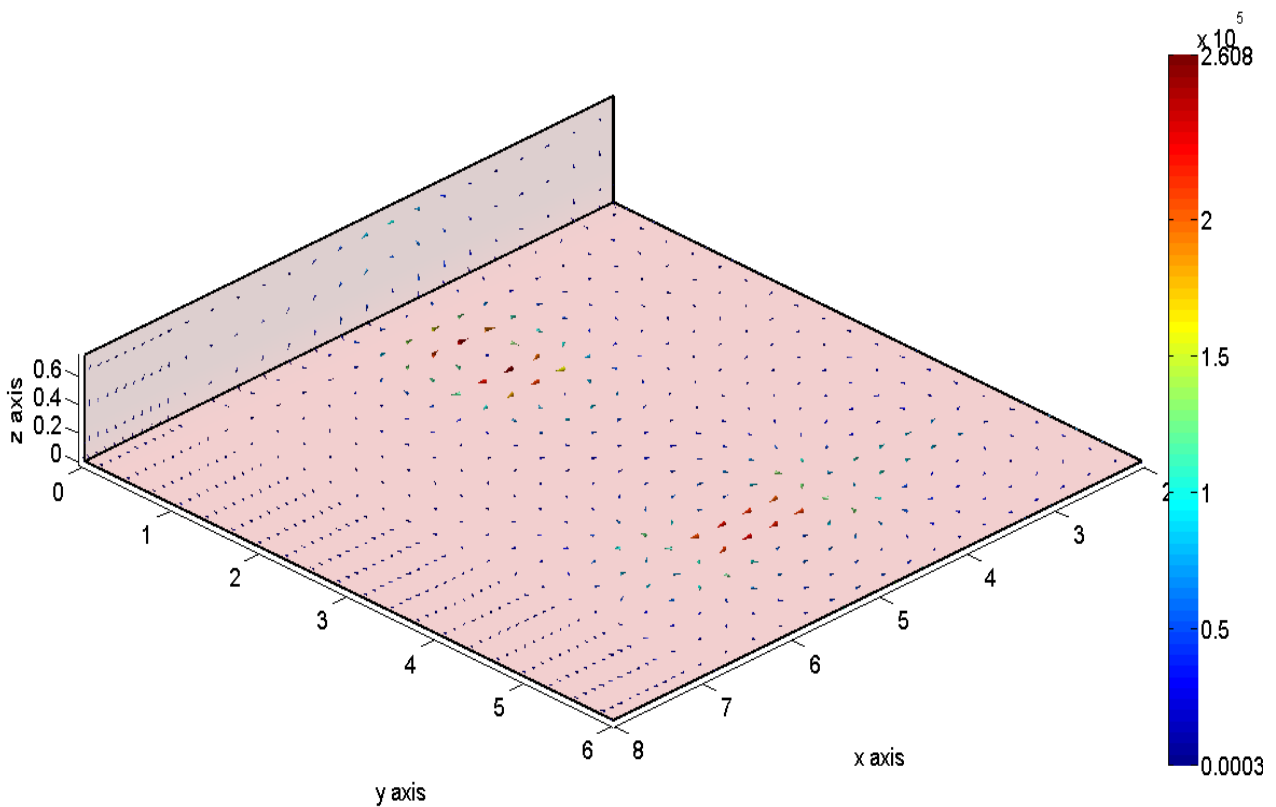

Figure 58 Results of the computation of the eddy currents, real part

Analyzing the results presented in Figure 58 we see that the higher values of the induced currents are in correspondence of transformer and low voltage switchgear. In particular, we note the strong influence of the columns of the transformer and the internal horizontal busbars of the low-voltage switchgear.
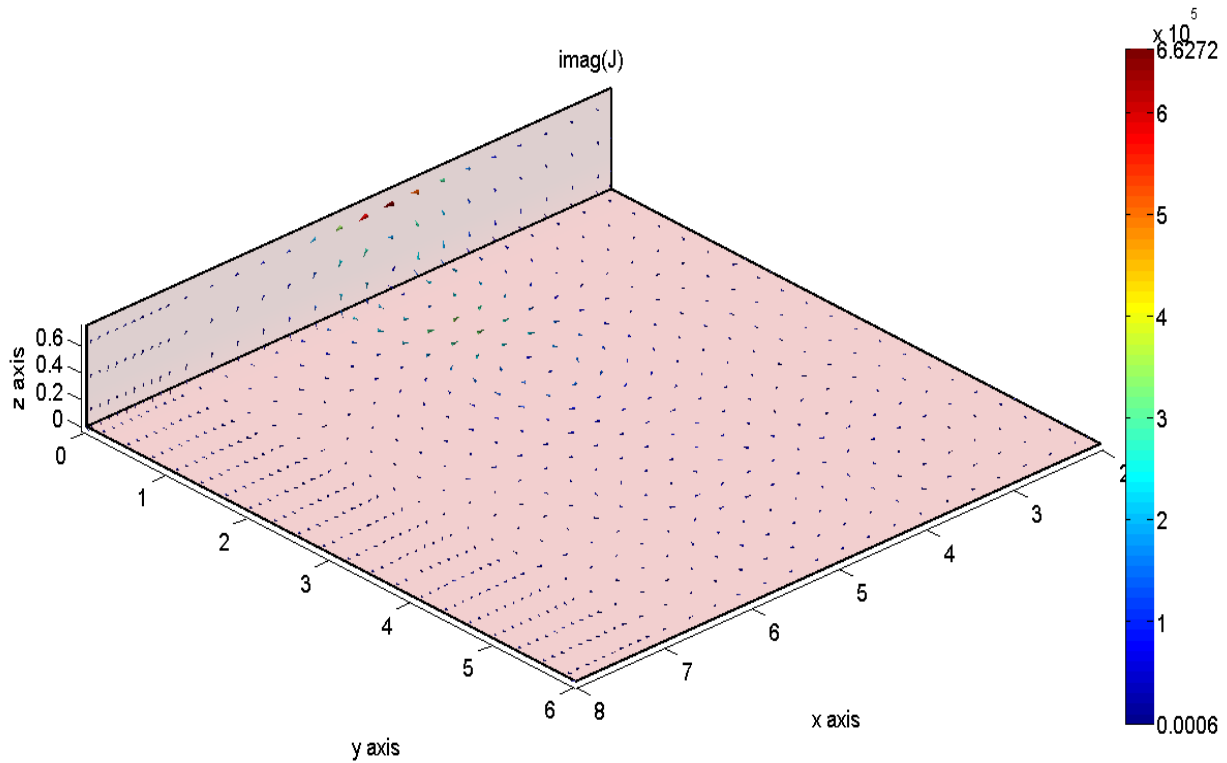
Figure 59 Results of the computation of the eddy currents, imaginary part

The shielding system allows to reduce the values of magnetic induction within the office area both at -1.6 m both at -3 m.

At the height of -3 m the goal is reached with a relatively high safety coefficient. The results obtained on a plane x-y with z= to -3 m are presented in Figure 61

In Figure 60 are show the map of magnetic induction calculated on a plane x-y at a coordinate z equal to -1.6 m with the shielding system positioned as show in Figure 57. The field map demonstrate that the values of magnetic induction are lower of 3 µT in all points and so the goal of the shielding system is reached.

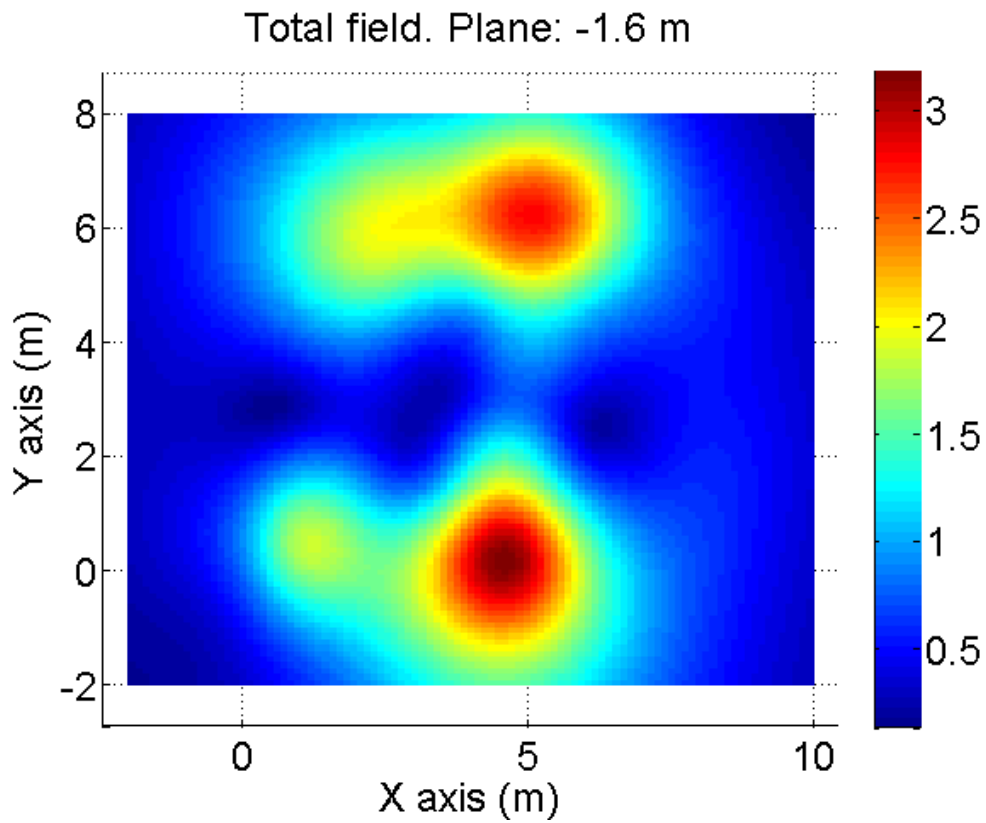**Figure 60 Field map in µT of the values of magnetic induction calculated on a plane x-y with z= -1,6 m after the positioning of the shielding system**
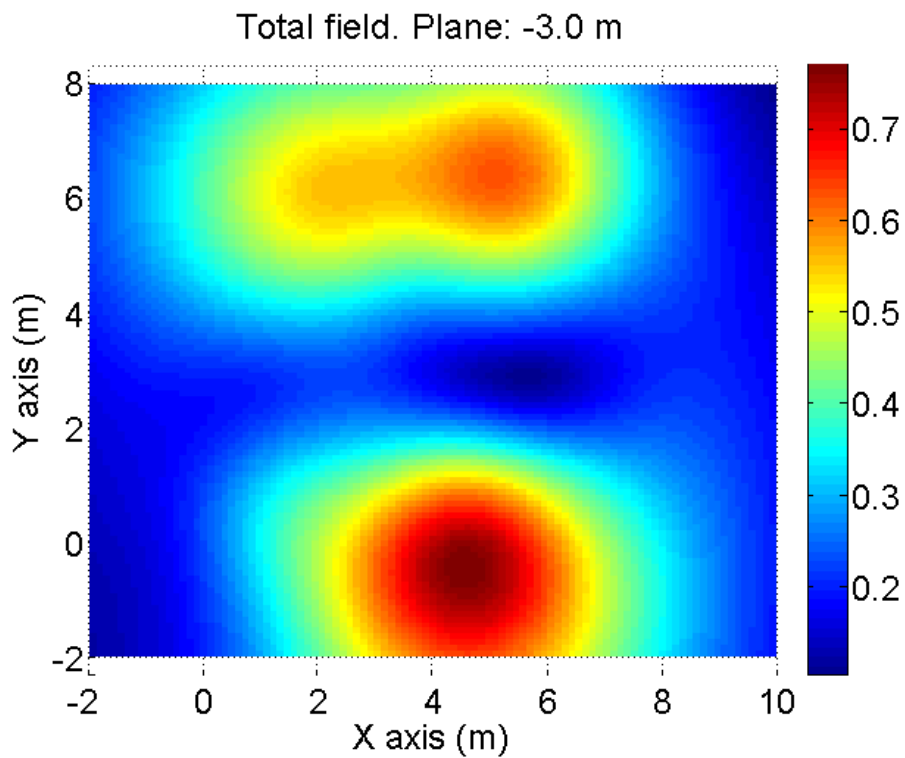

Figure 61 Field map in µT of the values of magnetic induction calculated on a plane x-y with z= -3 m after the positioning of the shielding system

Comparing the values of magnetic induction calculated in the absence of shielding with those calculated in the presence of shielding has been possible to extract the shielding factor that is reported in Figure 62 for the plane with z = -1.6 m and in Figure 63 for the plane with z = -3m.

The values of shielding result relatively high especially at the center of the shield.

The appendix placed on the wall behind transformers allows to minimize the end effect and in fact do not notice any strong discontinuity of the values of SF on the lower edge of the shielding system.
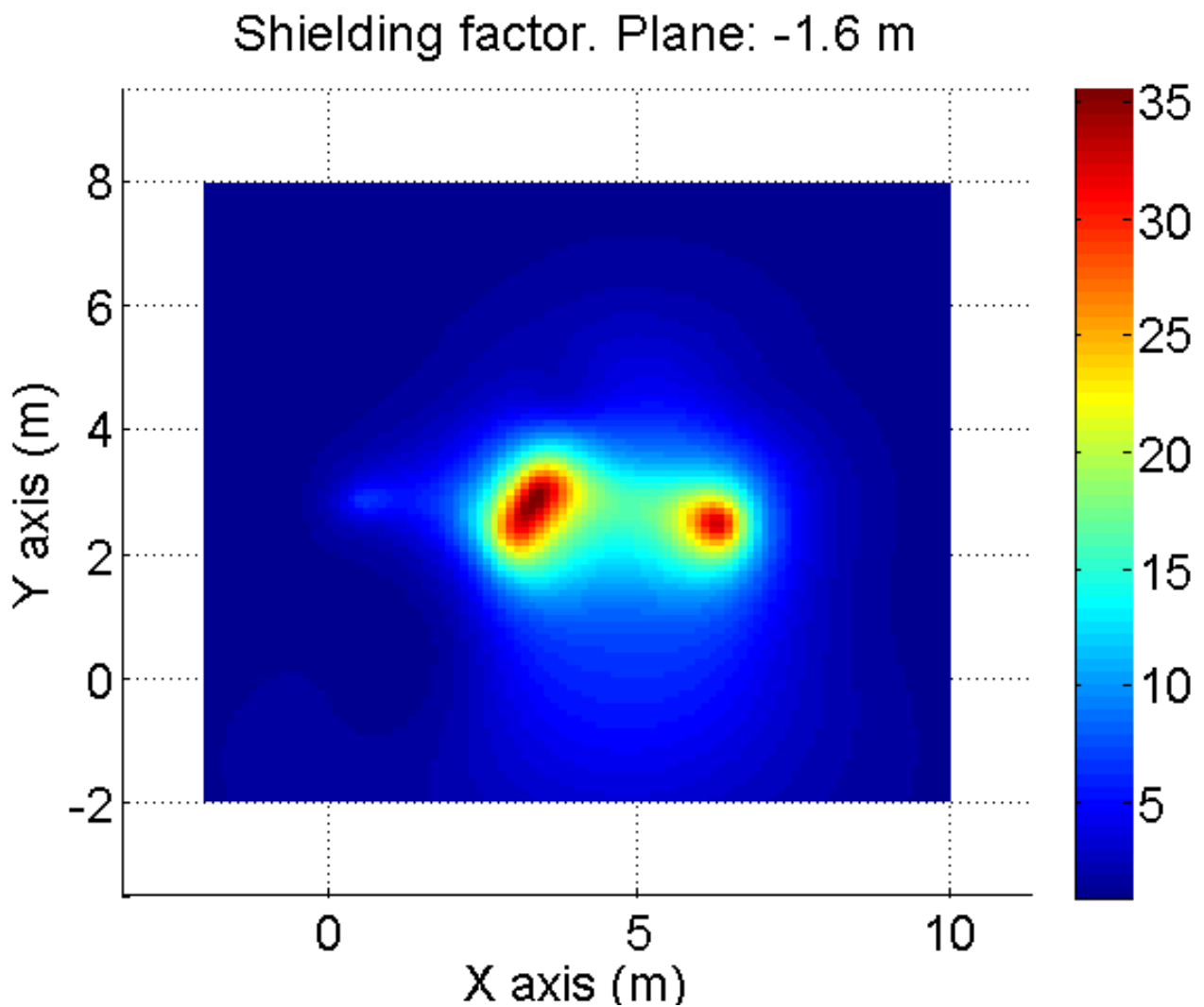

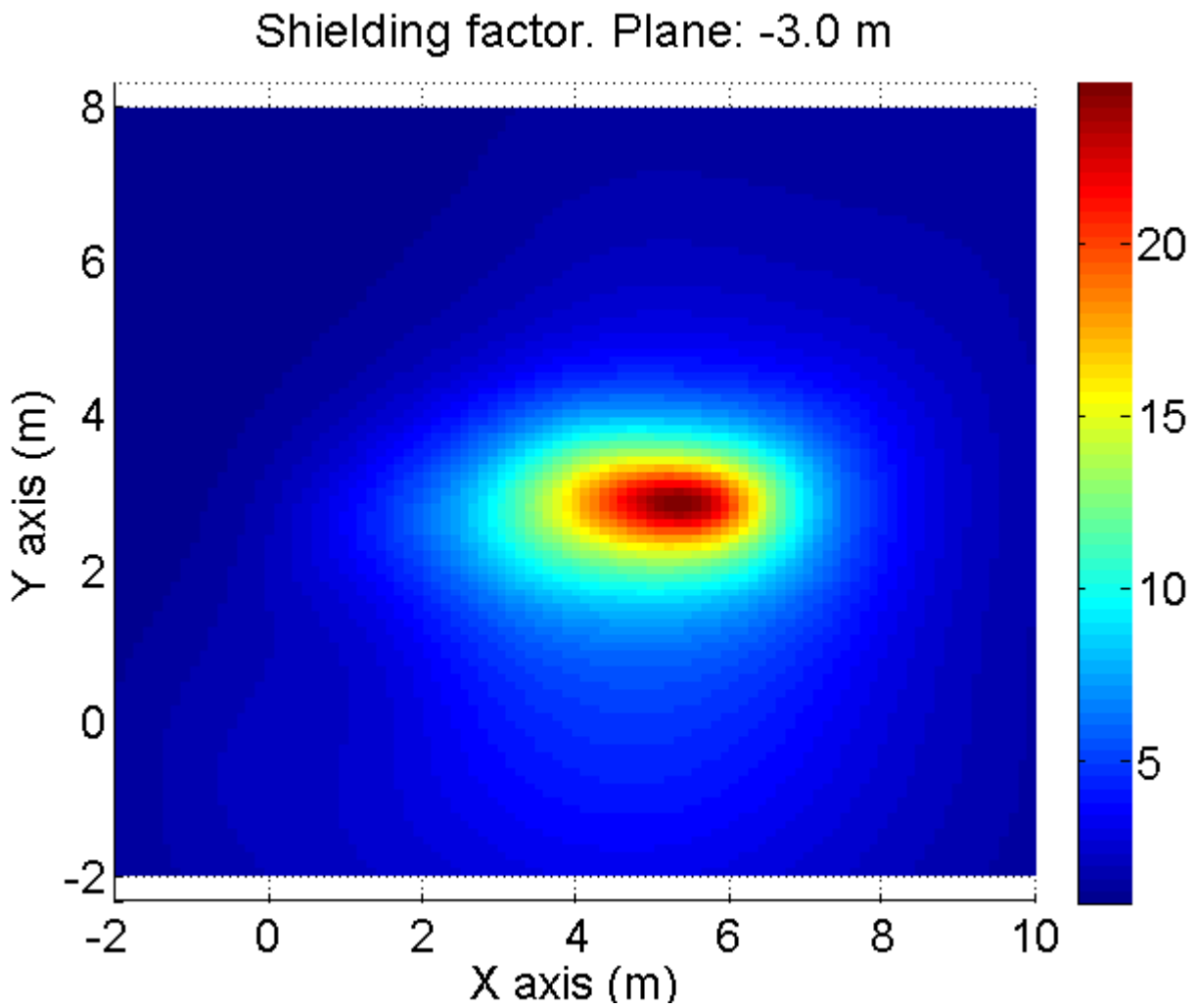Figure 62 Shielding factor provided to the shielding system on a plane x-y with z equal to -1.6 m

Figure 63 Shielding factor provided to the shielding system on a plane x-y with z equal to -3 m

The values of shielding factor obtain at the height of -3 m in correspondence of the center of shielding system are lower than those simulated at -1.6 m but in the other points of the analyzed plane are about the same.

4.3.4 Conclusion

The analyses presented in this chapter has focused on the study of a shielding system useful to reduce the values of magnetic induction produced by a MV / LV substation on the areas below it.

A conductive shielding system have been simulated.

The values of shielding factor provided by the shielding system are enough to achieve the objective of reduction of the values of magnetic induction under 3 μT on the entire x-y plane parallel to the floor of the substation and at the height z equal to -1.6 m.

Generally the value of SF is maintained relatively high even moving away from the shield.

The appendix placed behind the transformers allows to mitigate the end effect of the shield ensuring a shielding factor more homogeneous and the failure elevation of the values of magnetic induction at the edges.

4.4 Shielding of a typical MV/LV substation of the local distributor

In this section a shielding system for a typical MV/LV substation of the local distributor have been presented. The aim of this study is to design a shield able to contain the value of magnetic induction under 3 µT at no more than 0.5 m from the internal perimeter of the substation.

In contrast to the previous application, in this case, is not designed a complete shielding system but it is treated the study of a shield for each individual component of the substation. This allows, in most cases, to save shielding material and consequently money.

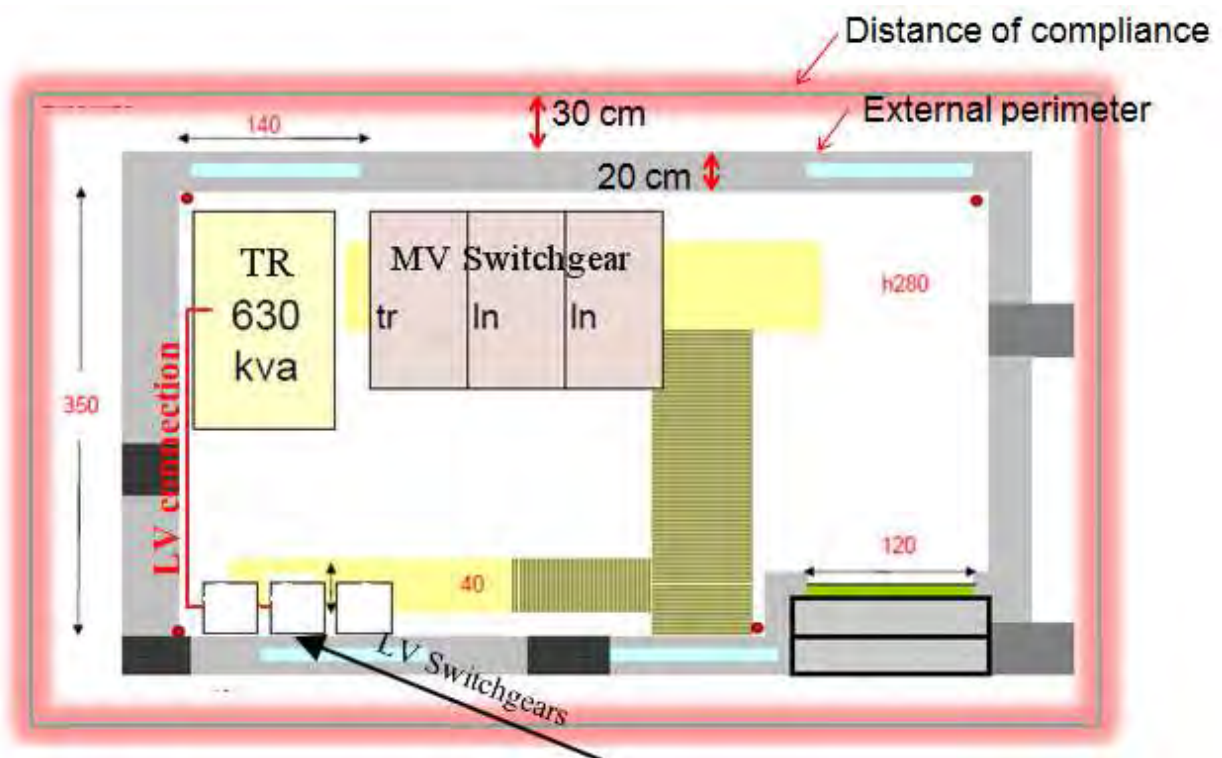The layout of a typical MV/LV substation is presented in Figure 64.

Figure 64 Layout of a typical MV/LV substation of the local distributor.

The devices of the substation take into account for this study are:

- An oil transformers MV/LV with power of 630 kVA
- Three low voltage switchgear consisting each one of two compartments
- A medium voltage switchgear consisting of three compartments
- A low voltage power lines composed of two conductor for each phase and other two for the neutral

4.4.1 Computation of the values of magnetic induction produced by the substation

In these analysis, at first, it is required to compute the so called distance of compliance (DOC), that is, the minimum distance from the source for having field levels lower than a given threshold. For these application the threshold is the value of 3 μT.

The MV/LV substation of the local distributor are different than the classic users substation because they have inside equipment specially designed for this application and therefore can not be used the standard models of the components.

In order to calculate the DOC without the shielding system the model of each component have been implemented.

➢ Integral model of the oil transformer

The model of the oil transformer has been split into two sub-models:

- Models of LV terminals/conductors

LV terminals and conductors can be accurately described by a straight current carrying wire. The wire is placed in the barycenter of the relative conductors so that the Biot-Savart law can be integrated along the straight conductor leading to a closed analytical expression for the magnetic field. It is worth noting that MV conductors can be introduced in the model with the same approach because it is independent from the voltage value. However, they are often neglected because close to the transformer their low level of current generates a negligible contribution to the overall magnetic field.

- Models of Primary and secondary windings

Primary and secondary windings are introduced in the model as massive coil with rectangular cross section. Therefore, each transformer column is composed by two of these windings as shown in Figure 6. The geometry of the windings is obtained from the actual geometrical data (DMV , DLV and Dax) and, equal and opposite ampere turns (N_1I_1, N_1I_2) are injected in the relative windings. The magnetic field of each column is calculated as presented in section 2.1.2.

The metallic enclosure of an oil transformer is generally made of steel and it strongly affected the values of magnetic induction generated by the winding. In order to take into account this influence

the shedding effect of the metallic enclosure is modelized by considering the magnetic properties of the material and by neglecting the possible eddy currents. The influence of the metallic enclosure is then evaluated using models of ferromagnetic shielding presented in section 2.3.1.

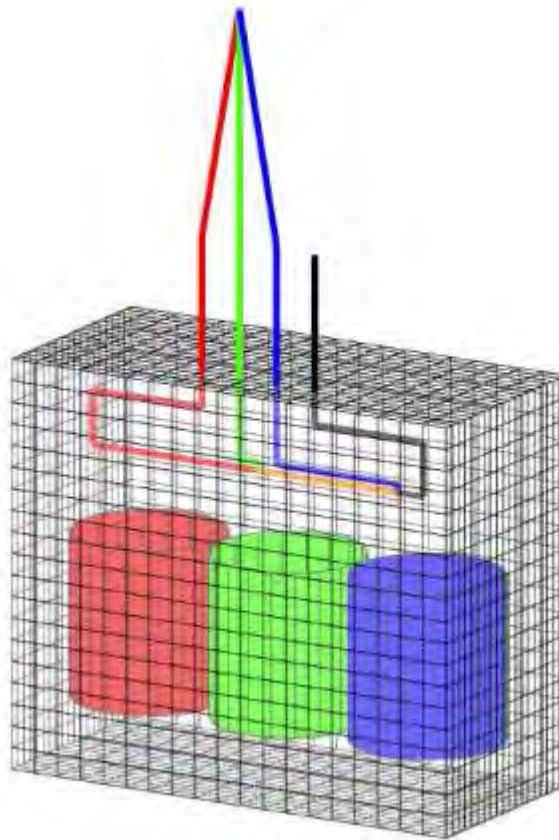The complete models of the oil transformer is show in Figure 65.

Figure 65 Transformer model

➢ Integral models of MV and LV switchgears

The approach used for MV and LV switchgears consists in building the geometry of the internal conductors, splitting them in several contiguous straight conductors, and applying the Biot-Savart law in order to calculate the magnetic flux density due to each segment. An example of MV and LV switchgears discretization is shown in Figure 66 (a) and Figure 66 (b) , respectively. The proposed model neglects the shielding effect of the metallic enclosure of the switchgear. Therefore, the use of this model to calibrate the simplified method assures some degrees of safety. However, it must be stressed that, the distance of compliance is often referred to very low magnetic field level (as 3 μT). Hence, it usually falls in the range of 2 to 4 m and. The effect of the metallic enclosure is quite negligible at these distances from the switchgears.
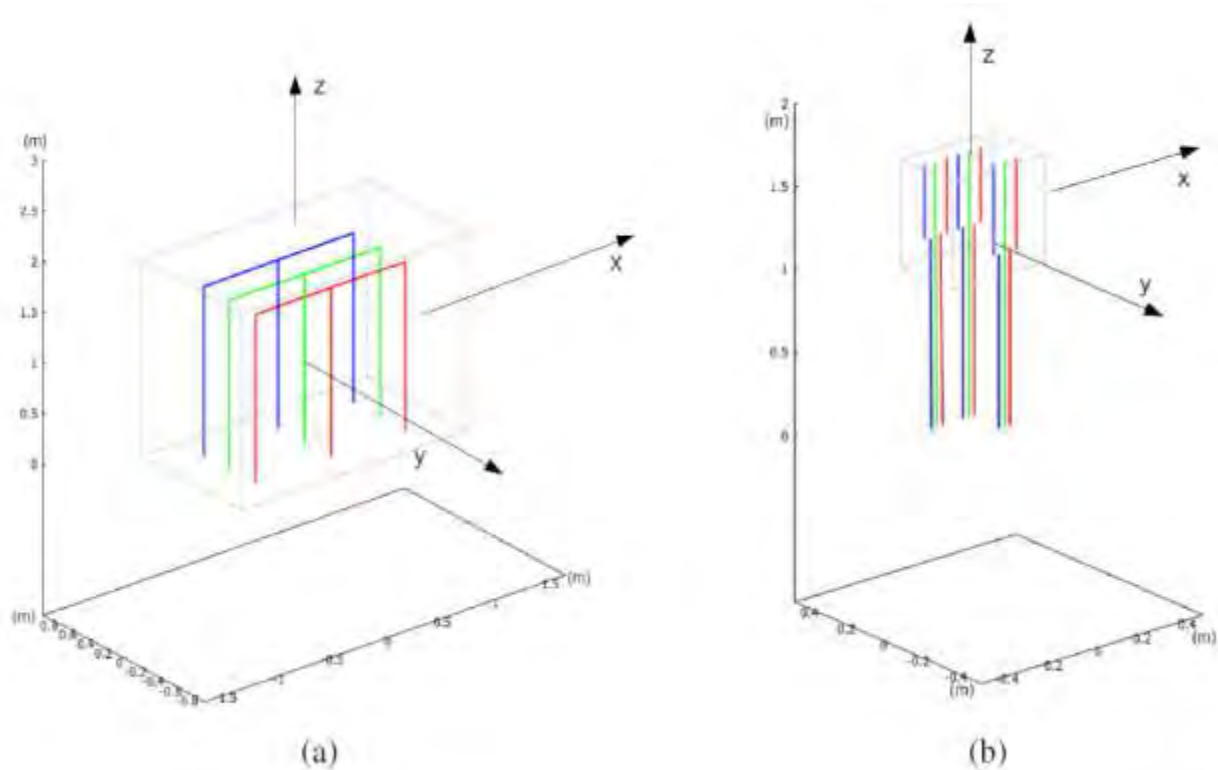
Figure 66 Subfigure (a) represents the 3D model of a three units MV switchgear: Unit n.1 and n.2 are arranged as ring-main, unit n.3 supplies a transformer. Subfigure (b) represents the 3D model of a LV switchgear with 2 circuit breaker.

The computation of the DOC is based on the superposition of the contemporary effects of all the field sources. As already said, it is defined as the isolevel curve related to the considered limit value, therefore, it is obtained by means of the solution of the complete 3D problem. As a first step, we highlight that in most of the practical configurations an approximated DOC can be computed with a superposition of the DOCs of each field source. In this regard, the standard configuration of MV/LV substation presented in Figure 64 is considered. The complete models of the substation is represented in Figure 67.

The inspection plane and the limit value must be chosen according the applicable regulatory framework. In this example we refer to the Italian one, hence, we compute the DOC related to a XY plane at 1 m from the ground level (z=1m). First of all the complete 3D problem is solved to obtain the rigorous DOC. Afterwards, each device is simulated separately in order to compute its own DOC. The overall DOC and the ones of each device are shown in Figure 68.

It is apparent that the global DOC is well approximated by the envelope of the curves related to the single DOCs. This result relies on the low interaction among the sources that is true only if they are separated by enough space. However, this is a really compact substation, therefore, it is highly unlikely that the distance between the devices could be much shorter. For this reason, in the

following we describe a simplified procedure that is based on the superposition of DOCs that are obtained considering the sources separately.
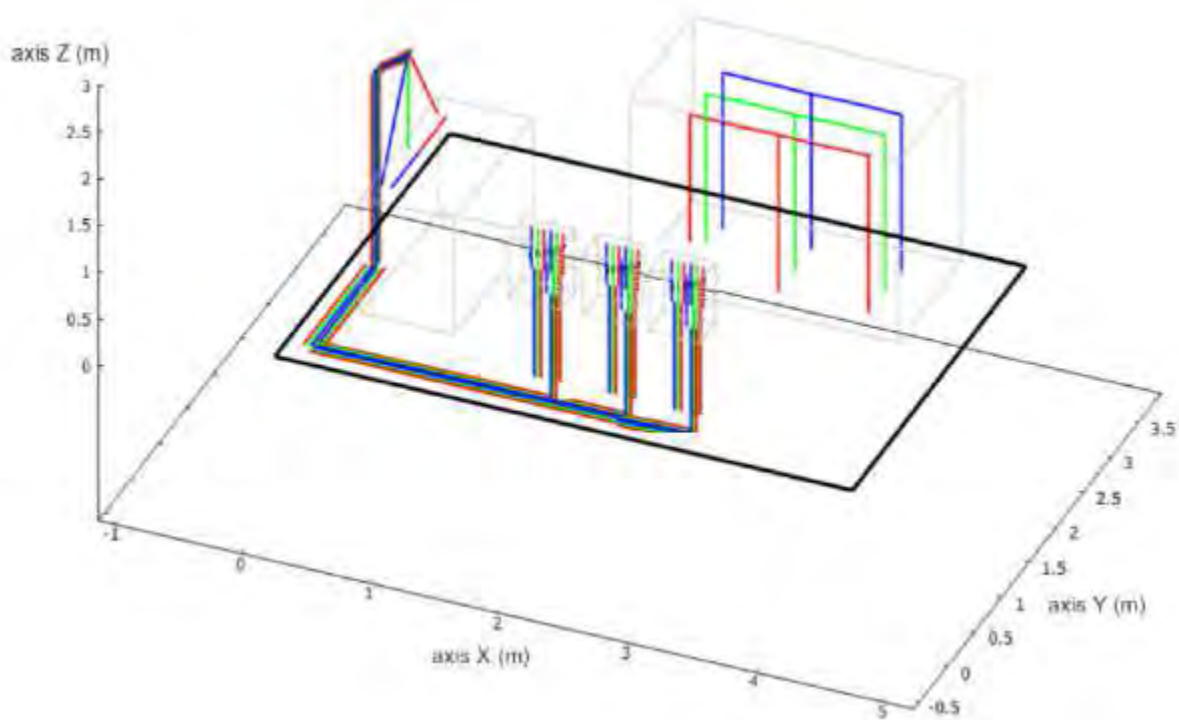

Figure 67 3D layout of the standard MV/LV substation adopted by the Italian electricity distributor
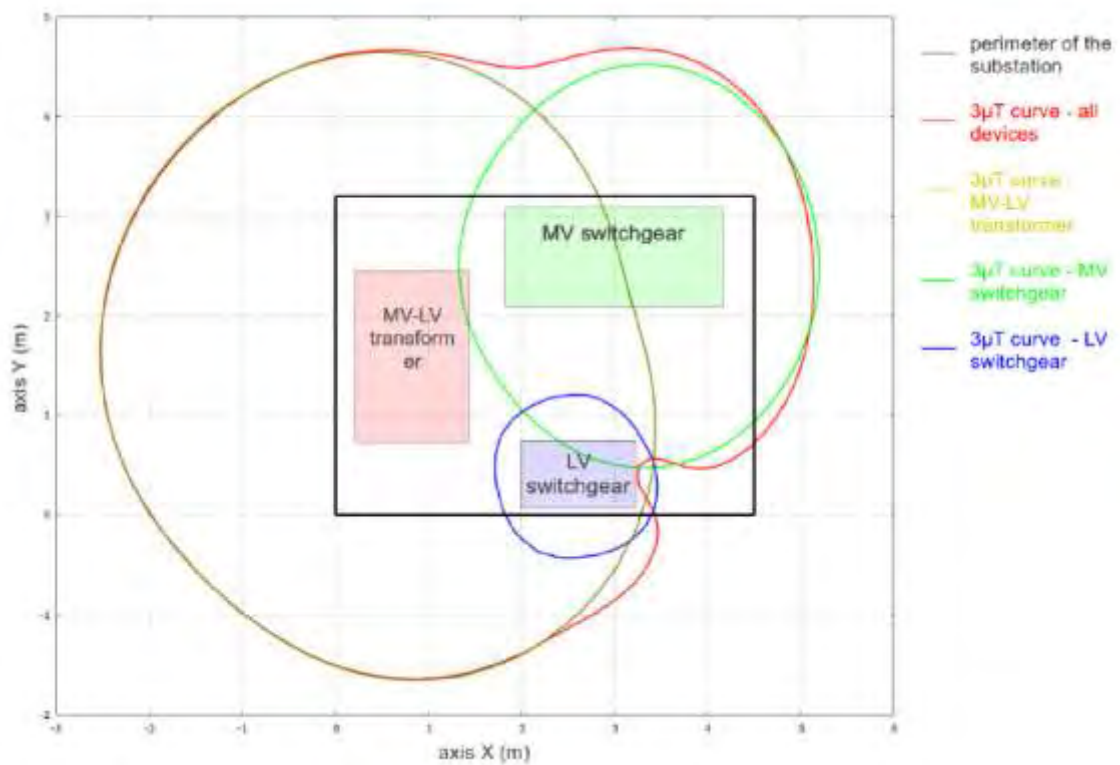

Figure 68 Global isolevel curve 3 μT (red curve), and single isolevel curves 3 μT for each device in substation.

4.4.2   Validation of the sources models

Before showing the results of the study of shielding systems of each component is interesting to show the results obtained by the validation of computational models.

➢   MV/LV Oil Transformer

The magnetic field emission of a 630 kVA oil transformer 15kV=400V is investigated by means of measurements. In Figure 69 (a) a picture of the system is reported. Moreover, as shown Figure 69 (b) the LV terminals are short circuited by means of three massive conductors in order to take into account the magnetic field emission of LV power line close to the transformer. The transformer is tested at its rated values of primary and secondary current. The power of the system have been provided by the system described in 3.2.

(a)   (b)

Figure 69 (a) Experimental investivation of the magnetic field emission is carried out on a 630 kVA oil transformer (15 kV=400 V) (b) LV terminals are short circuited by means of three massive conductors

The same configuration is analyzed with the proposed integral technique in order to verify its accuracy. In Figure 65 the 3D model is shown, it is possible to observe the three columns, the LV

connections and the discretization of the metallic enclosure. In order to compare measurements and simulations two inspection lines are identified as shown in Figure 70. They are both located at 1 m from the ground level and, particularly, Line 1 includes frontal and posterior points whereas line 2 is defined by some lateral points.
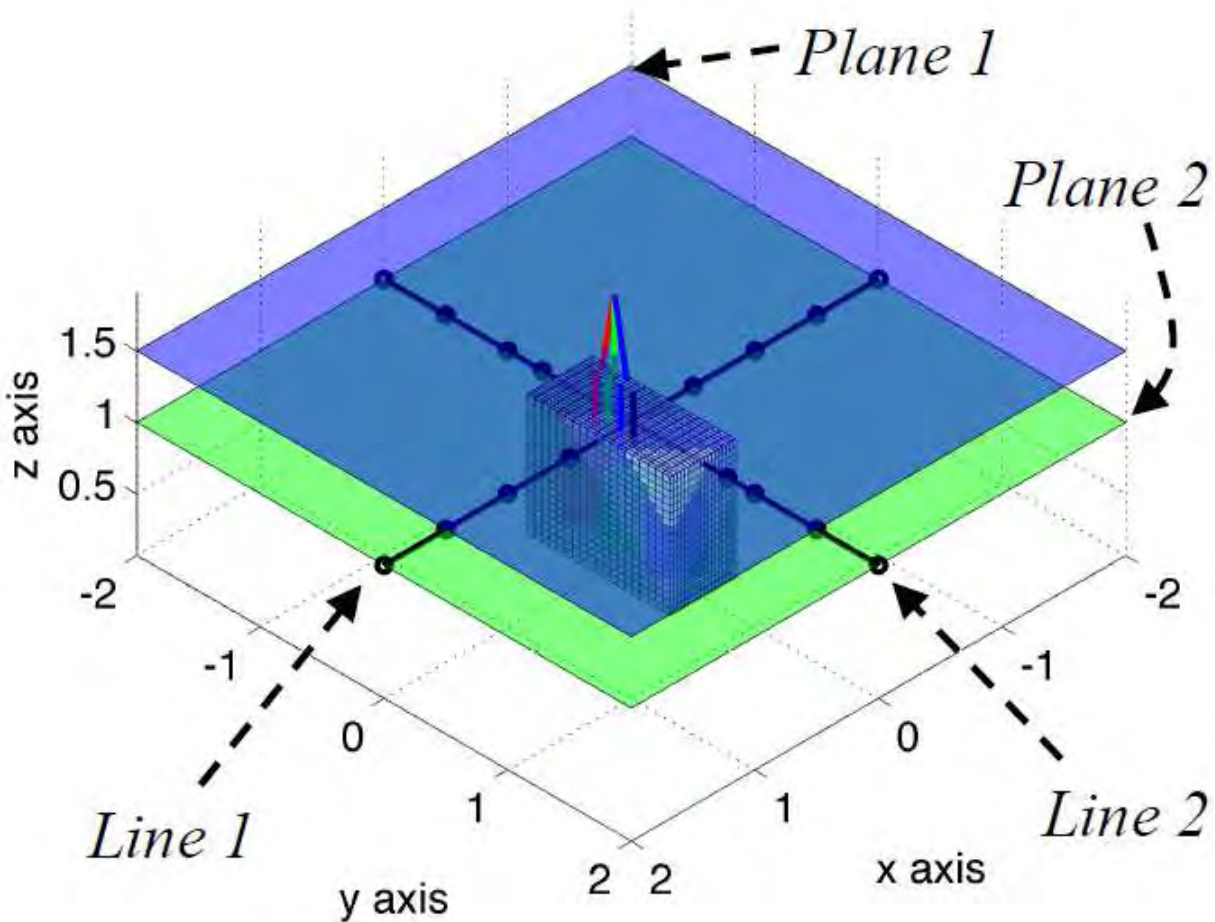

Figure 70 inspection lines and inspection planes. Line 1 includes frontal and posterior points whereas line 2 is defined by some lateral points. Plane 1 and plane 2 are located at 1 m and 1.5 m far from the ground level, respectively.

Moreover two inspection planes are defined to compare the isolevel curves related to the values 3 μT and 10 μT (these values are of particular importance in the Italian regulatory framework). Plane 1 and plane 2 are located at 1 m and 1.5 m far from the ground level, respectively. Firstly, the model is calibrated identifying the relative permeability of the ferromagnetic material. The calibration is carried out by minimizing the error between simulation and measurement along the line 1. Assuming a relative permeability (μ_r) equal to 550 a good result is obtained as shown in Figure 71. Moreover, the value of the identified permeability is in the correct order of magnitude for the commonly employed metallic material.
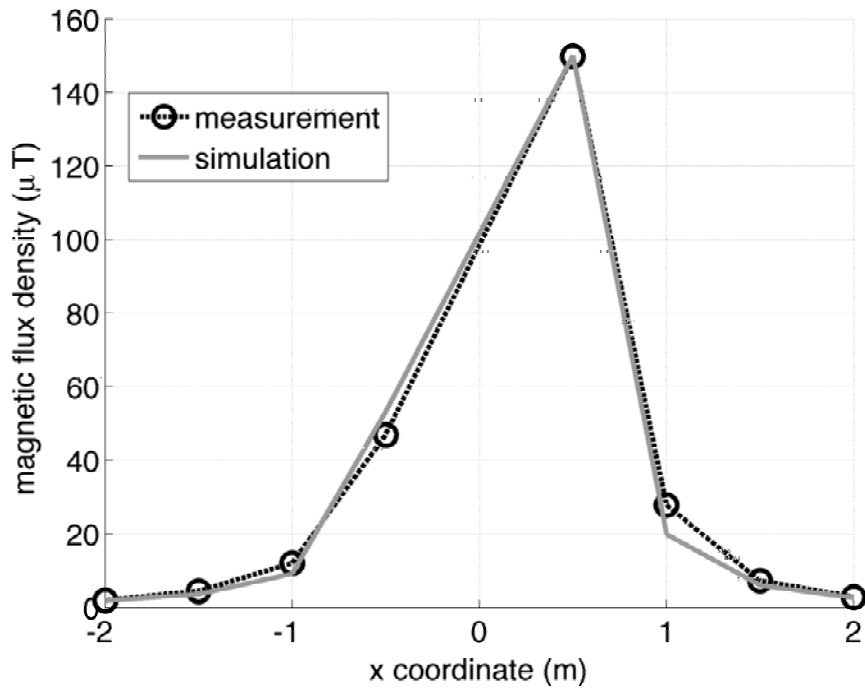
Figure 71 Measurement vs. simulation over the inspection line 1

The same value of μ_r is used for the other comparisons. In Figure 72 simulations and measurements along line 2 are shown. It is apparent that the model is still in good agreement with the measured values.
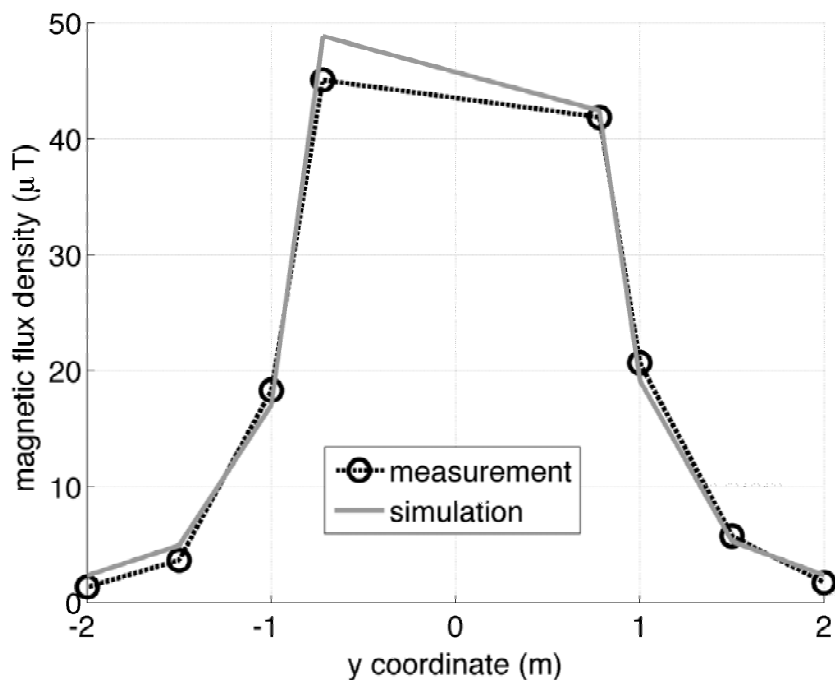

Figure 72 Measurement vs. simulation over the inspection line 2

93

Finally, in Figure 73 and Figure 74 the isolevel curves related to 3 µT and 10 µT are shown. Thinner and wider lines are correspond to simulations and measurements, respectively.
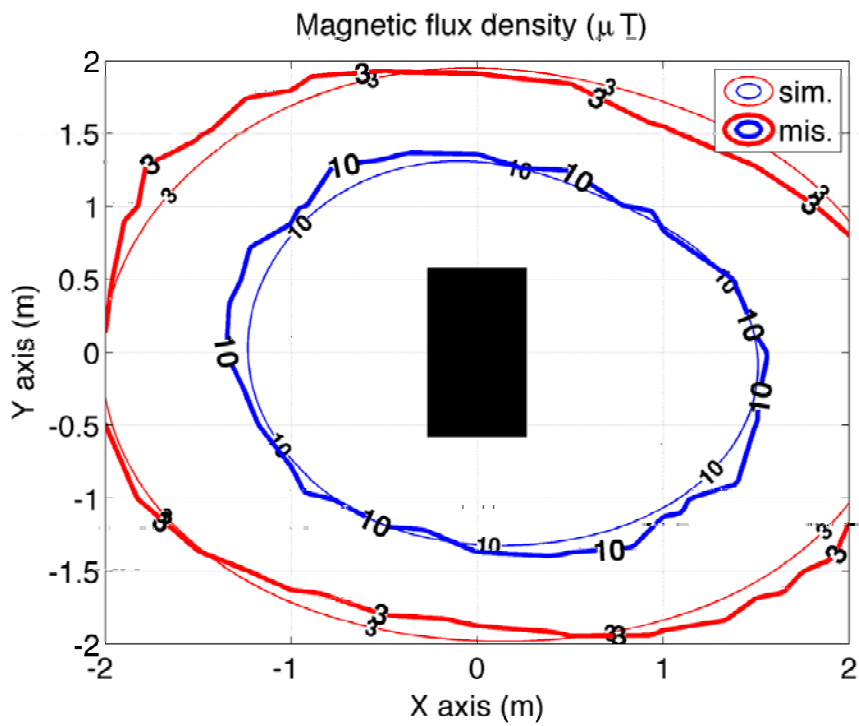
Figure 73 Comparison on Plane 1: isolevel curves at 3 µT and 10 µT: thinner lines for simulations and wider lines for measurements
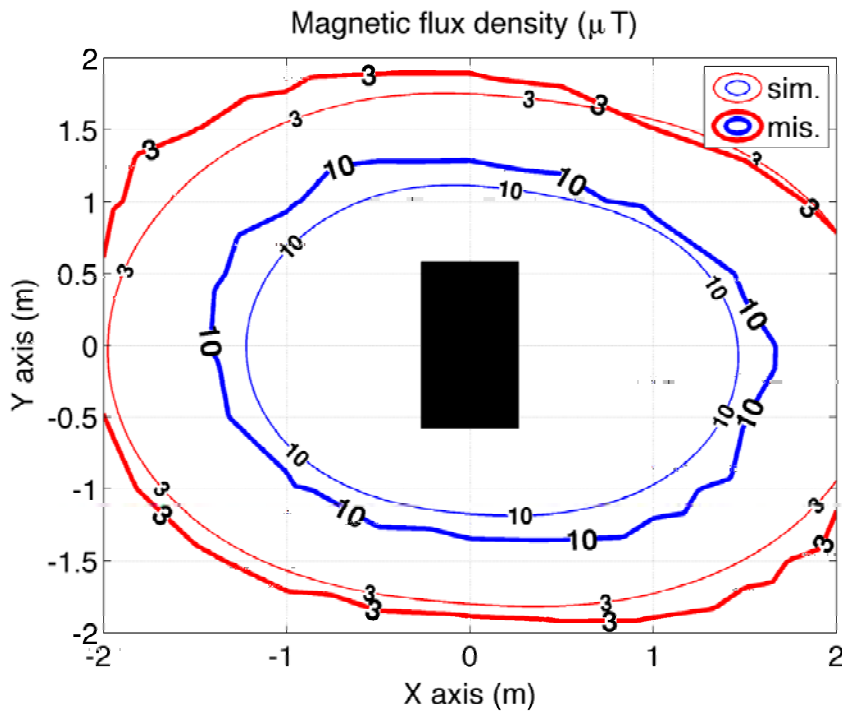
Figure 74 Comparison on Plane 2: isolevel curves at 3 µT and 10 µT: thinner lines for simulations and wider lines for measurements

The comparisons highlighted a good agreement between simulations and measurements confirming that the employed simplification hypotheses are acceptable in this context.

➢ MV switchgears

The validation of the model of the MV switchgear are easier because the enclosure is so thin to not affect the magnetic induction generate by these two sources.

The switchgear has been tested at his nominal current: of 300 A (value valid for the configuration as ring-main).

The alimentation for the tests have been provided using the generator described in section 3.1. The imagine of the laboratory test are presented in Figure 75 .

Figure 75 Image of the test on the MV switchgear

The test have been carried out closing in short circuit the output terminals of the device as show in Figure 76

Figure 76 image of the short circuit connection of the terminal of the MV switchgear.

For the MV switchgear the values of magnetic induction have been measured on two different plane x-y located at 1 m and 2 m far from the ground level. The results of the measurements and of the computation are presented respectively in Figure 77 for the plane at 1m and in Figure 78 for the plane at 2 m.
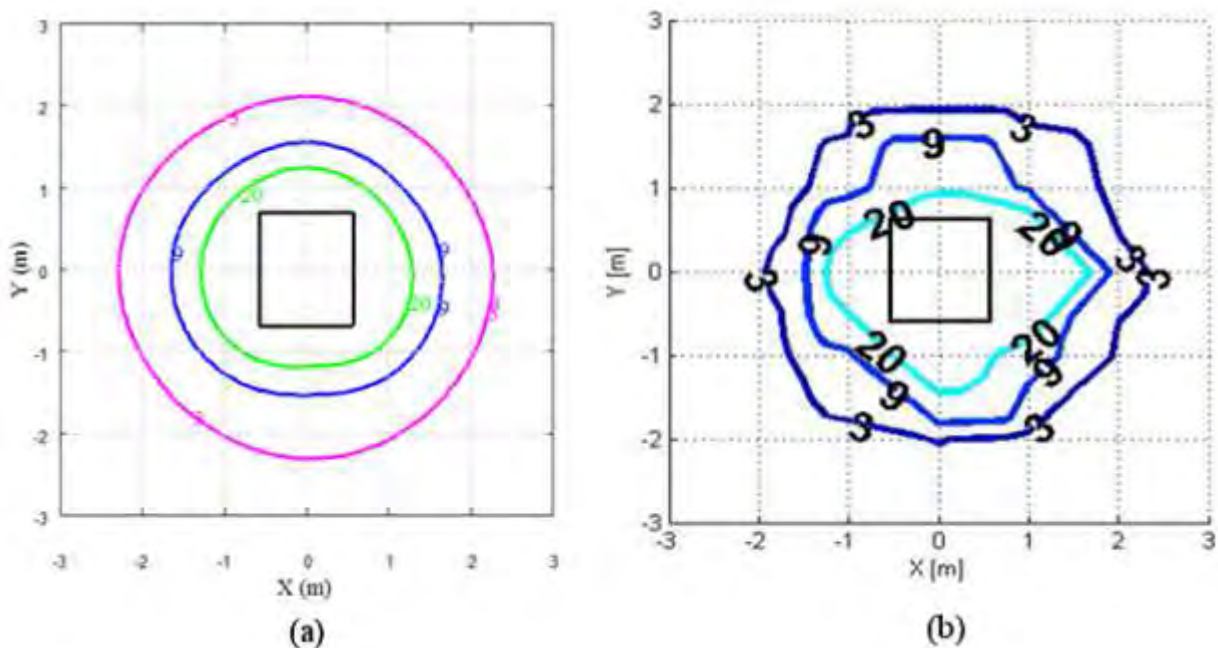

(a)

(b)

Figure 77 Comparison on a plane x-y with z =2m, isolevel lines relative at the computed (a) and measured (b) values of magnetic induction generate by the MV Switchgear
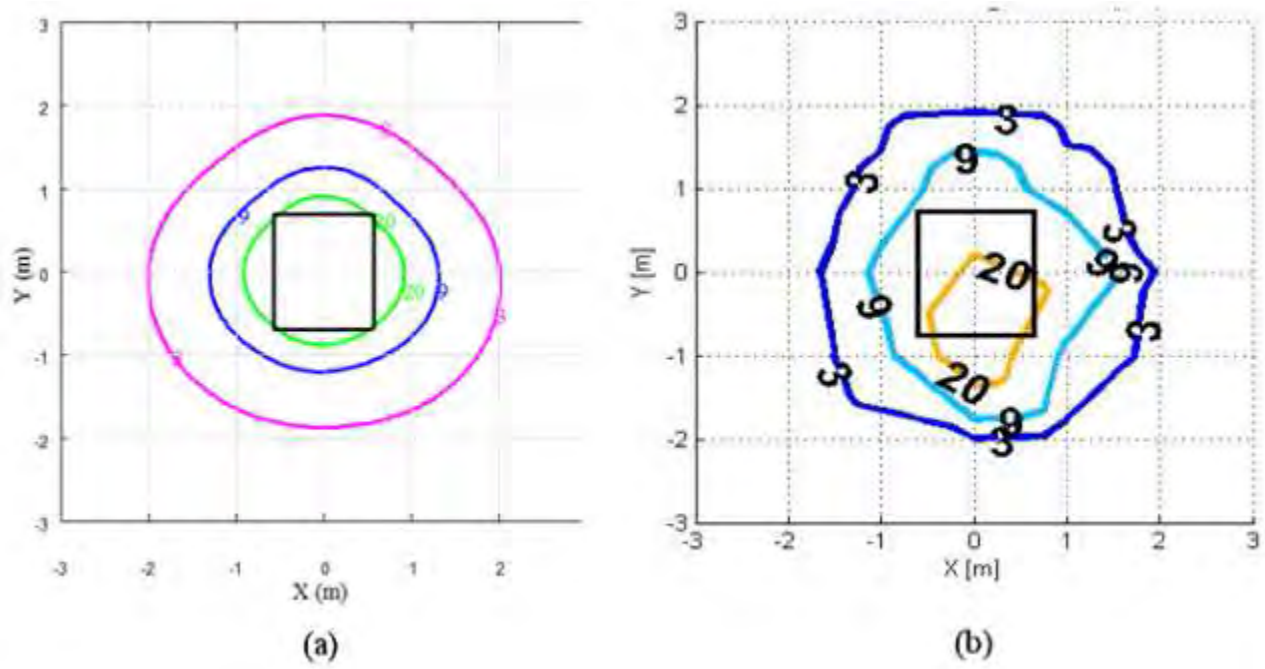
Figure 78 Comparison on a plane x-y with z =2m, isolevel lines relative at the computed (a) and measured (b) values of magnetic induction generate by the MV Switchgear

From the results presented in Figure 77 and in Figure 78 it is clear that the values of magnetic induction computed and measured are very close. The only differences between the measured values and those calculated are probably due to the influence supply to the switchgear.

4.4.3 Design of the shielding system

For each component listed before the design of the shield was carried out using a conductive material.

The property of any shielding system and of the sources are reported below.

➢ MV/LV Oil transformer, 630 kVA:

- Electrical conductivity = 35 MS/m
- Relative magnetic permeability $\mu_r = 1$
- Thickness of the shield = 3 mm
- Transformer operating at his rating power (current of 909 A)
- Layout of the shielding system presented in Figure 79
- Distance of the transformer from the shield: 50 cm for each sides
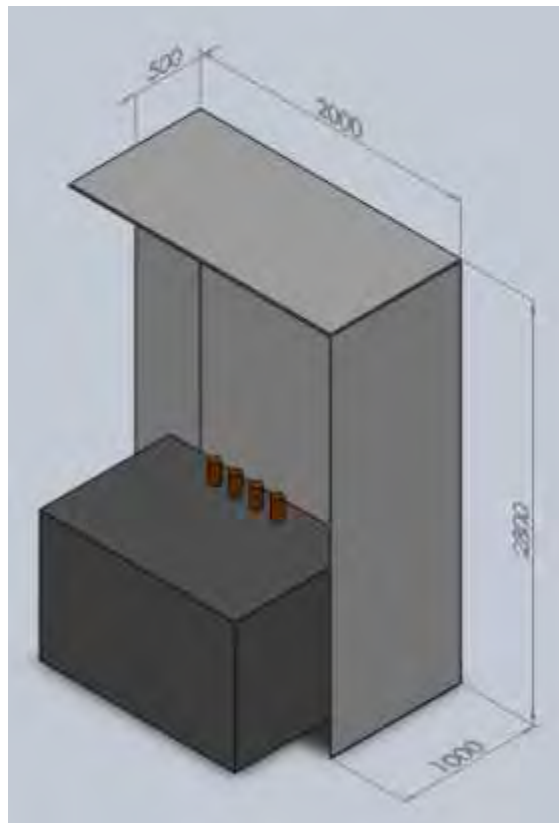
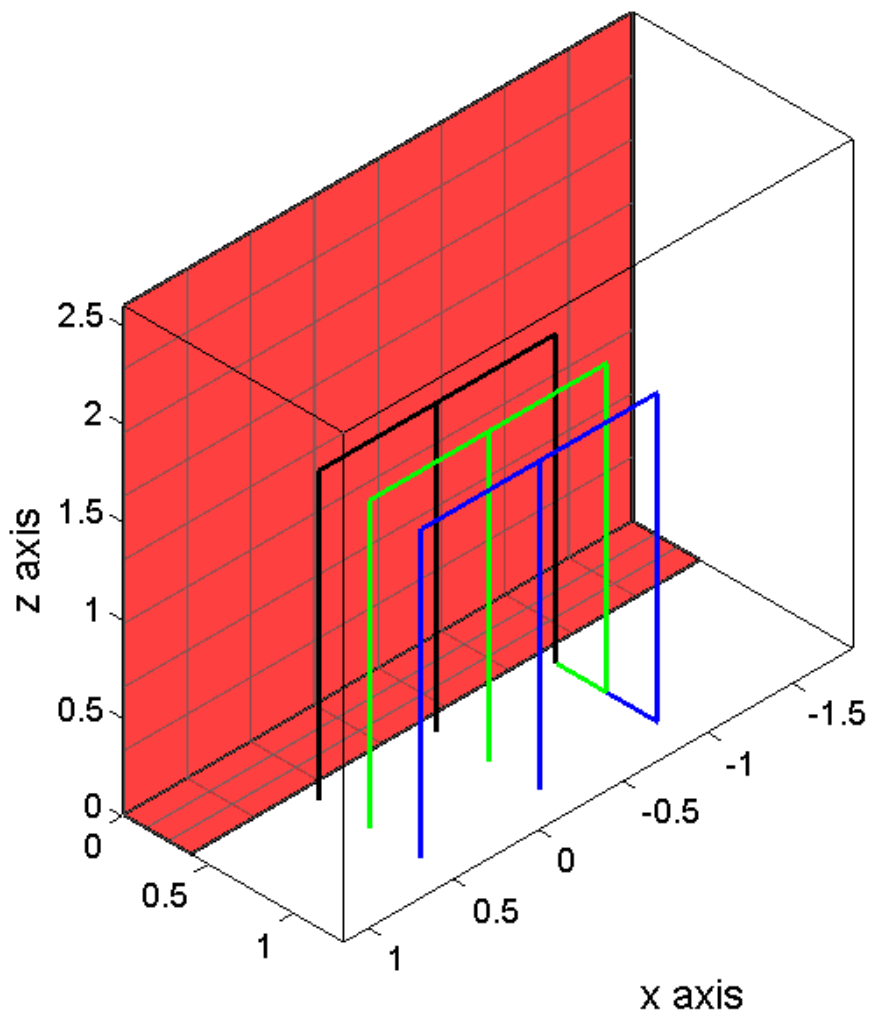
Figure 79 Layout of the shield designed for the MV/LV transformer

➢ MV Switchgear

- Electrical conductivity = 35 MS/m
- Relative magnetic permeability $\mu_r = 1$
- Thickness of the shield = 3 mm
- MV switchgear with three compartments
- Two compartments in ring-main configuration operating at the nominal current of the ring equal to 300A
- A compartment for the alimentation of the transformer with current equal to the nominal MV current of the transformer (about 25 A)
- Layout of the shielding system presented in Figure 80
- Distance of the MV from the shield: 20 cm

Figure 80 In red the layout of the shield designed for the MV Switchgear

➤ LV Switchgear

- Electrical conductivity = 35 MS/m
- Relative magnetic permeability $\mu_r = 1$
- Thickness of the shield = 3 mm
- Three LV switchgear operating each one with a current equal to 303 A with circuit
- Two circuit breakers for each LV switchgear (current of 151.5 A for each circuit breakers)
- Layout of the shielding system presented in Figure 81
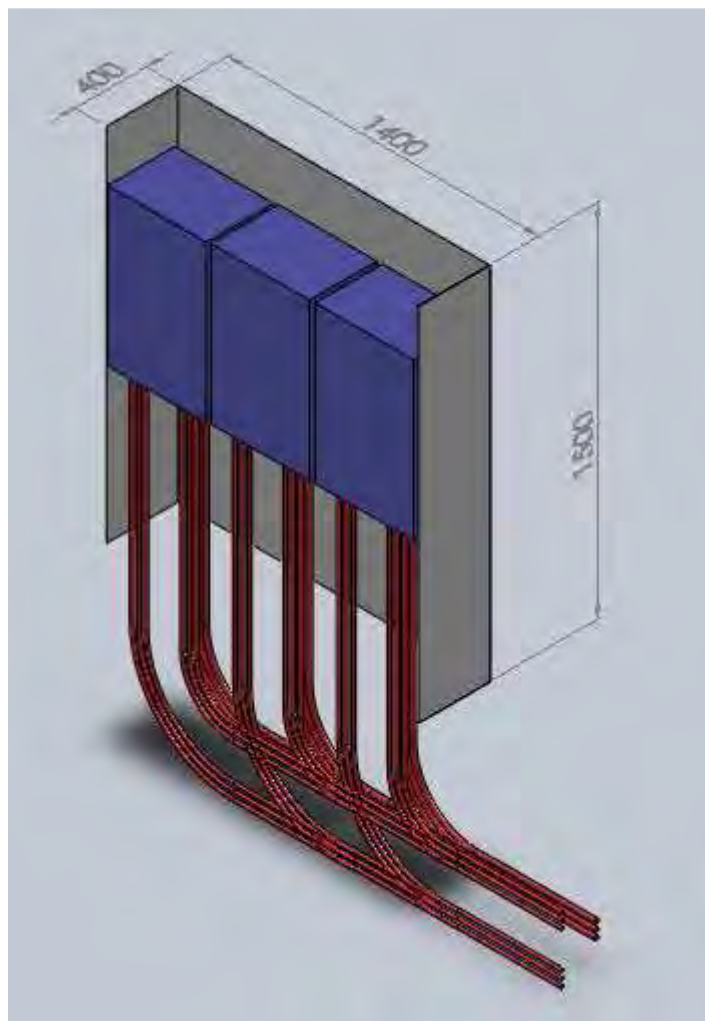- Distance of the LV from the shield: 10 cm

Figure 81 In gray the layout of the shield designed for the LV Switchgear

4.4.4 Result of the simulations

The simulation have been carried out using the models of the component described before and a shielding system have been designed for each component in order to reach the goal set. In this paragraph the results obtained with the simulations are presented.

➢ MV/LV Oil transformer, 630 kVA:

In the classical layout of a MV/LV substation of the local distributor presented in Figure 64 the transformer is placed on a corner of the substation and so the shielding system have been designed in order to protect by magnetic fields generated on both sides bordering to the external. The values of magnetic induction have been calculated on two different planes show in Figure 82 (a) (x-z plane) and in Figure 82 (b) (y-z plane).
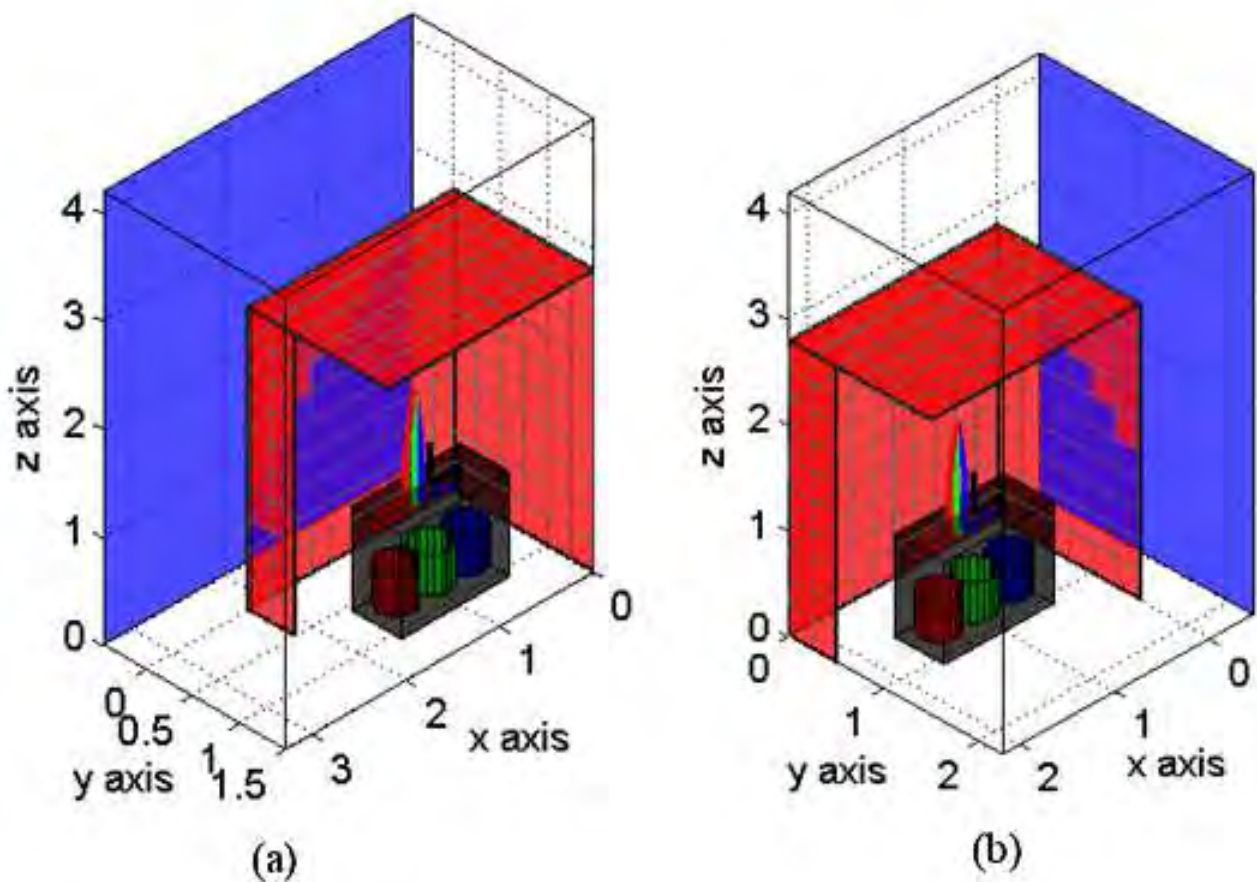
Figure 82 Layout of the shielding system (in red) with the computation planes (in blue): (a) x-z plane, (b) y-zplane

At first the computation of the values of magnetic induction generate by the transformer, without the shielding system, was performed. The results are presented respectively in Figure 83 for the x-z plane and in Figure 84 for the y-z plane.
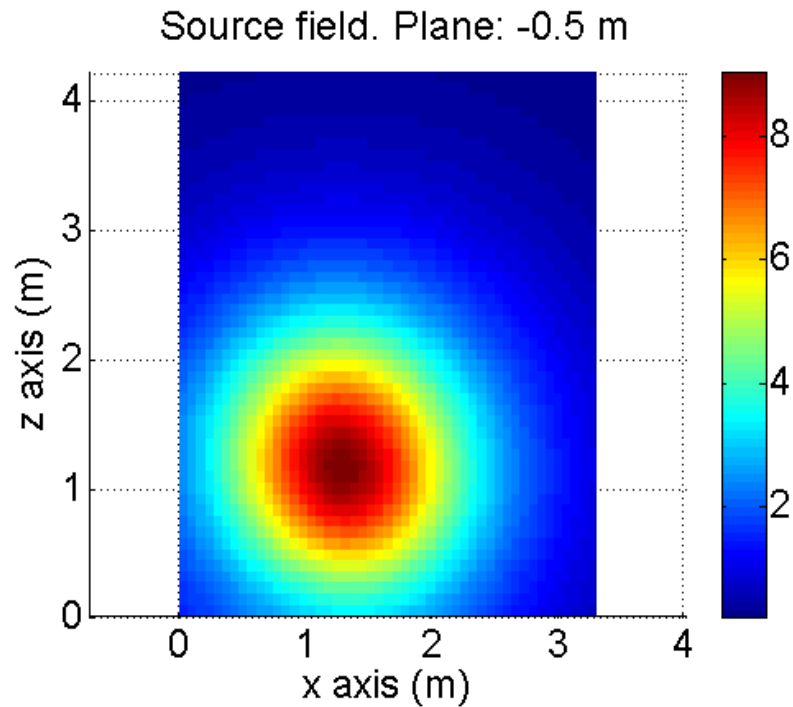

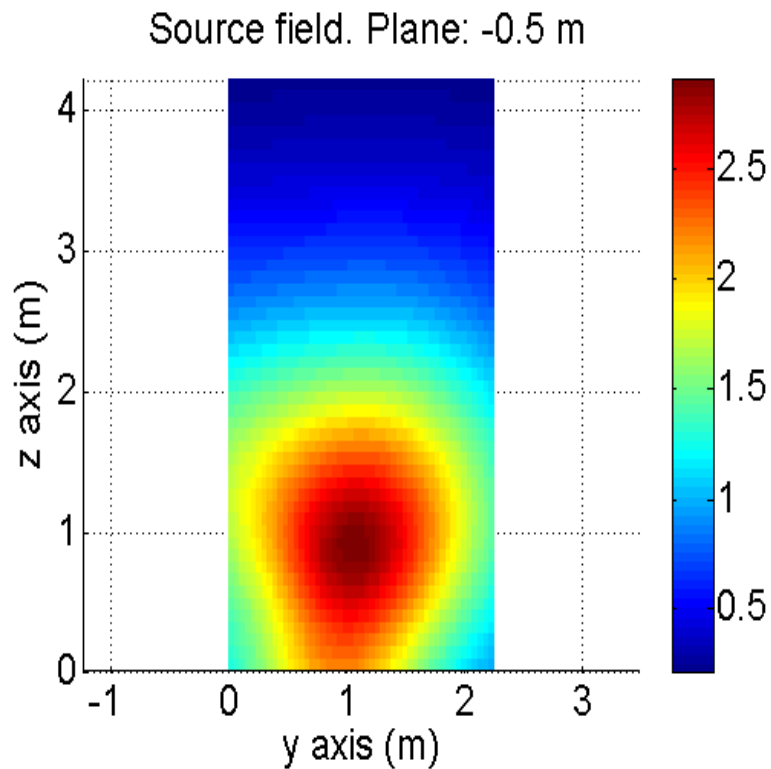**Figure 83 Field map in µT of the computed values of magnetic induction generated by the transformer on the x-z plane**

Figure 84 Field map in µT of the computed values of magnetic induction generated by the transformer on the y-z plane

With the shielding system the values of magnetic flux density is reduced as shown in Figure 85 for the x-z plane and in Figure 86 for the plane y-z.
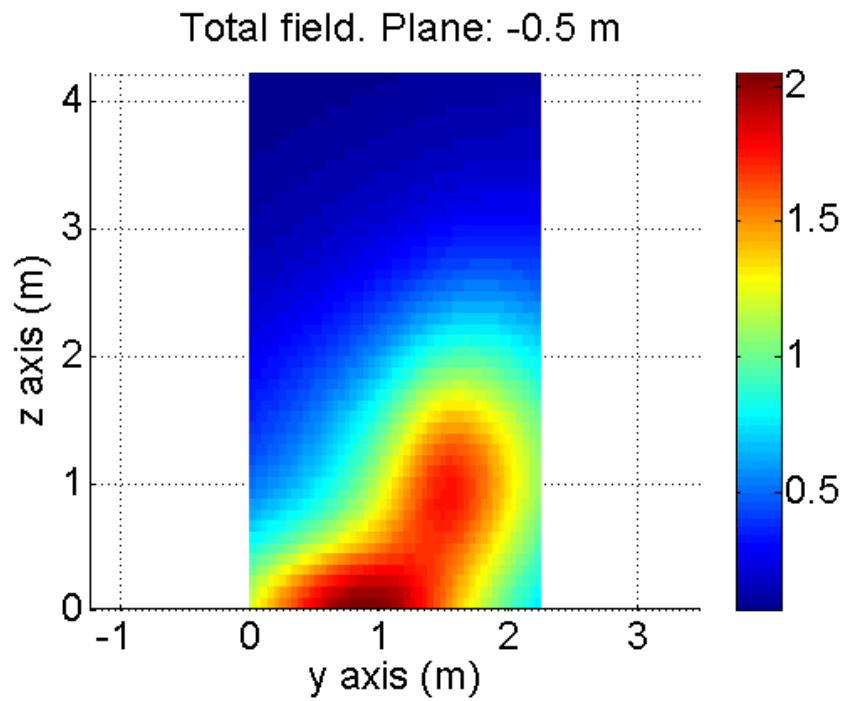
Total field. Plane: -0.5 m

Figure 85 Field map in µT of the computed values of magnetic induction generated by the transformer on the x-z plane after the positioning of the shielding system
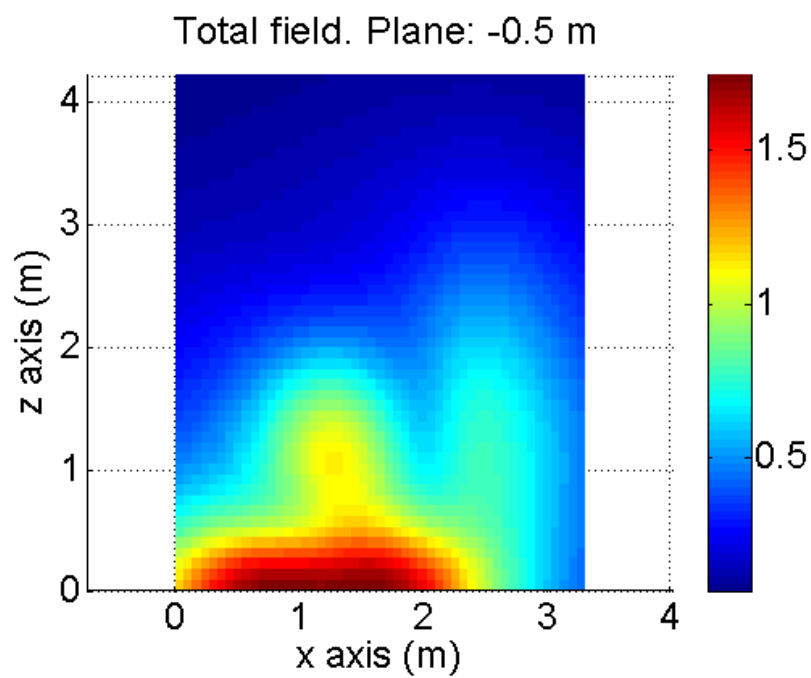
Total field. Plane: -0.5 m

Figure 86 Field map in µT of the computed values of magnetic induction generated by the transformer on the y-z plane after the positioning of the shielding system

From the results presented is simple to verify the shielding factor achieved with the installation of the shield. The results of this calculation are presented respectively Figure 87 for the x-z plane and in Figure 88 for the y-z plane.
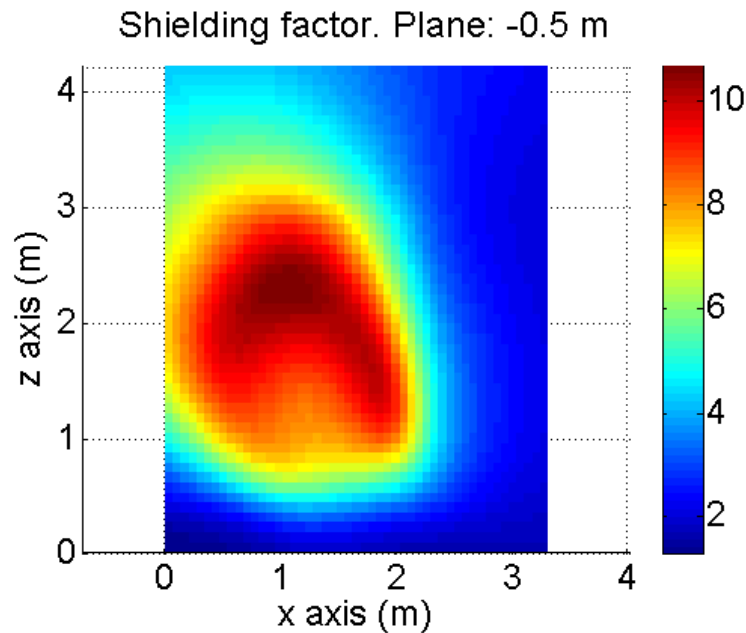

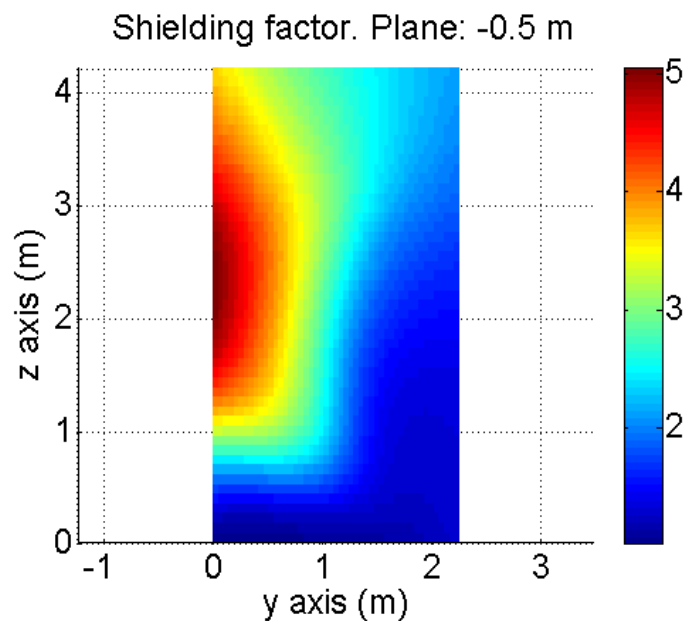**Figure 87 Field map of the SF achieved on the x-z plane**

Figure 88 Field map of the SF achieved on the y-z plane

Analyzing the results presented in the previous figures we can see how, with the installation of the shield, relevant shielding factors are obtained (even greater than 9). The values of magnetic induction are therefore, with a good coefficient of security, below the limit of 3 μT.

➢ MV Switchgear

As shown in Figure 68 the MT switchgear generate values of magnetic induction higher than the target set only on the wall parallel to the x axis , and therefore in this case is analyzed only a calculation plane x-z. The position of the computation planes relative to the shield is reported in Figure 89.
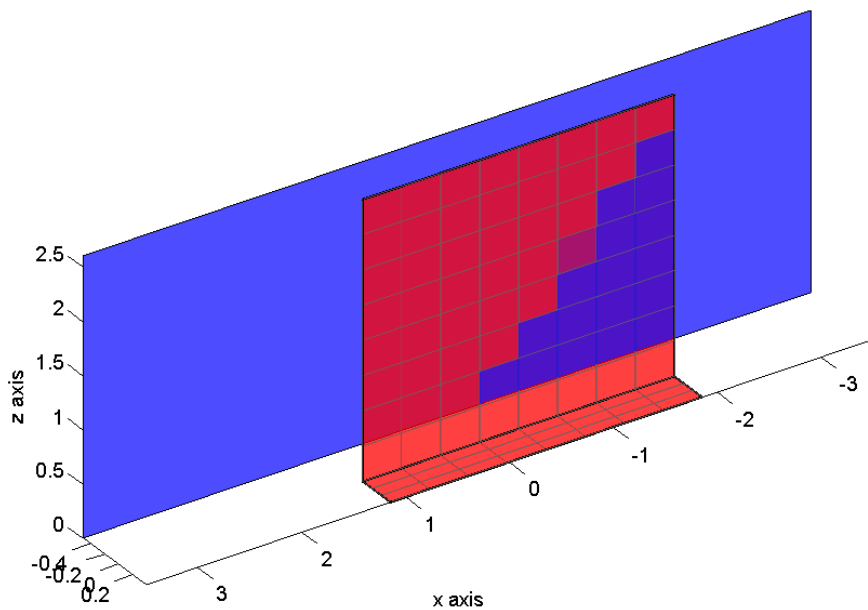

Figure 89 Layout of the shielding system (in red) with the computation planes (in blue)

The computation of the values of magnetic induction generate by the MV switchgear, without the shielding system, is presented in Figure 90
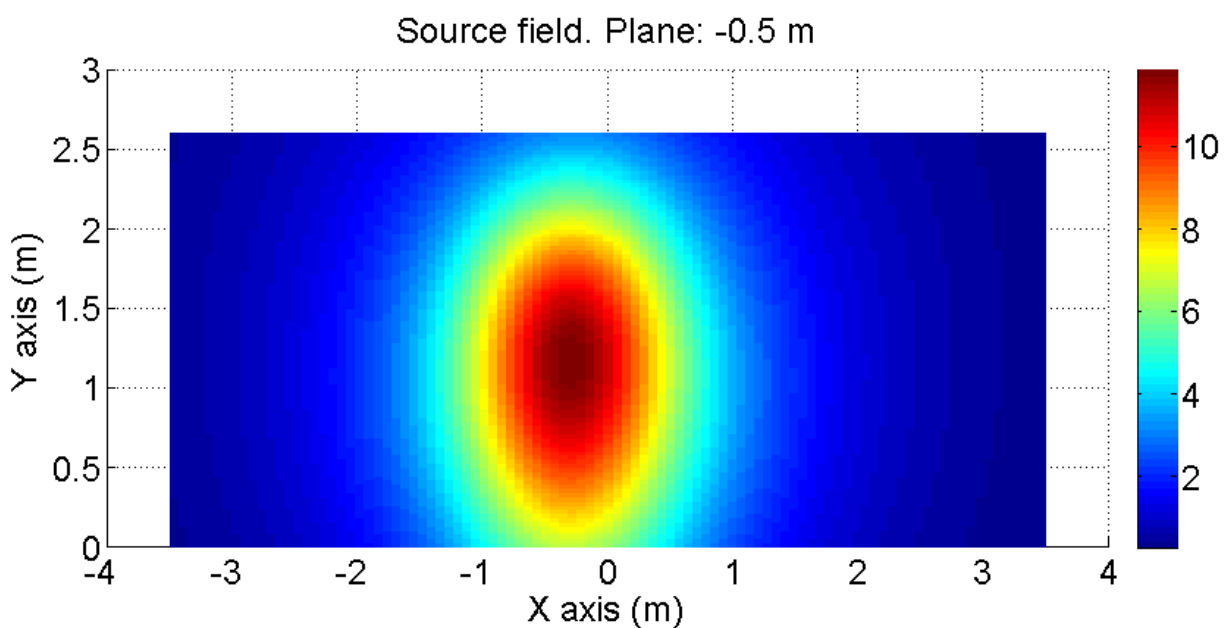

Figure 90 Field map in µT of the computed values of magnetic induction generated by the MV switchgear on the x-z plane